

Mass Determination and Detection of the Onset of Chromospheric Activity for the Sub-Stellar Object in EF Eridani

Steve B. Howell¹, Frederick M. Walter², Thomas E. Harrison³,
Mark E. Huber⁴, Robert H. Becker^{4,5}, Richard L. White⁶

ABSTRACT

EF Eri is a magnetic cataclysmic variable that has been in a low accretion state for the past nine years. Low state optical spectra reveal the underlying Zeeman-split white dwarf absorption lines. These features are used to determine a value of 13-14 MG as the white dwarf field strength. Recently, 5-7 years into the low state, Balmer and other emission lines have appeared in the optical. An analysis of the H α emission line yields the first radial velocity solution for EF Eri, leading to a spectroscopic ephemeris for the binary and, using the best available white dwarf mass of $0.6M_{\odot}$, a mass estimate for the secondary of $0.055M_{\odot}$. For a white dwarf mass of $0.95M_{\odot}$, the average for magnetic white dwarfs, the secondary mass increases to $0.087M_{\odot}$. At EF Eri's orbital period of 81 minutes, this higher mass secondary could not be a normal star and still fit within the Roche lobe. The source of the Balmer and other emission lines is confirmed to be from the sub-stellar secondary and we argue that it is due to stellar activity. We compare EF Eri's emission line spectrum and activity behavior to that recently observed in AM Her and VV Pup and attributed to stellar activity. We explore observations and models originally developed for V471 Tau, for the RS CVn binaries, and for extra-solar planets. We conclude that irradiation of the

¹WIYN Observatory and National Optical Astronomy Observatory, 950 N. Cherry Ave, Tucson, AZ 85719
howell@noao.edu

²Dept. of Physics and Astronomy, Stony Brook University *fwalter@astro.sunysb.edu*

³New Mexico State University *tharriso@nmsu.edu*

⁴IGPP/Lawrence Livermore National Laboratory, Livermore, CA 94550 *mhuber@igpp.ucllnl.org*

⁵Dept. of Physics, University of California at Davis, Davis, CA 95616

⁶Space Telescope Science Institute, 3700 San Martin Dr., Baltimore, MD 21218

secondary in EF Eri and similar systems is unlikely and, in polars, the magnetic field interaction between the two stars (with a possible tidal component) is a probable mechanism which would concentrate chromospheric activity on the secondary near the sub-stellar point of the white dwarf.

Subject headings: stars: activity — stars: low-mass, brown dwarfs — stars: individual (EF Eri, AM Her, VV Pup)

1. Introduction

EF Eridani has become a binary star of renewed interest in recent years. This is primarily due to the fact that the mass accretion from the low-mass secondary to the highly magnetic white dwarf has been essentially stopped for the past 9 years. During this period of very low accretion, observers have flocked to telescopes around the world in hope of detecting and understanding the component stars that make up EF Eri. As we will see, it has taken a small 1.5-m telescope, part of the SMARTS consortium, to provide the first new insights into the true nature of this fascinating (and confounding) binary.

EF Eri was discovered over 30 years ago as a hard X-ray source (2A 0311 -227; Cooke et al. 1978). It was quickly identified optically as a 14th magnitude blue source (Griffiths et al. 1979) with properties similar to AM Herculis (Charles and Mason 1979). AM Her, the not-so-typical prototype of the AM Her class of interacting binaries, was the first member of a new class of cataclysmic variable (Tapia 1977). Today, these magnetic cataclysmic variable (CV) binary systems are called polars (due to their polarized light), systems in which matter is accreted onto the more massive primary from the lower mass secondary. The primary star is a highly magnetic white dwarf ($B \sim 10$ MG to 250 MG) and the mass donor ranges from normal M stars (as in AM Her) to sub-stellar brown dwarf-like objects which are believed to reside in EF Eri and other ultra-short period CVs (see Warner 1995 for a review).

Polars show large, random changes in their brightnesses on weeks to months, and even year timescales. In the high state, when mass accretion is in full swing, their luminosities are dominated by an accretion-produced continuum from the X-ray to the IR, superposed with strong emission lines from hydrogen and helium. When the mass transfer slows or stops, the underlying stars are revealed, and these dominate the optical and infrared spectral energy distribution. The origin for the starting and stopping of the mass transfer from the low mass companion is not understood, but stellar activity cycles in the synchronously locked, rapidly spinning late type secondary has been a long standing explanation (see Bianchini, 1992; King and Cannizzo 1998; Hessman et al. 2000) which has recently gained some observational

support (Kafka et al. 2005, 2006; Mason et al. 2006).

A number of recent papers have been dedicated to EF Eri (e.g., Beuermann et al. 2000; Harrison et al. 2003, 2004) and they track the evolution of this system into its low state, where the system evolved to the point where the optical spectrum was emission-line free, and dominated by a cool white dwarf that showed Zeeman-split Balmer absorption lines (e.g., see Fig. 2 in Harrison et al. 2004). The secondary in EF Eri has not yet been conclusively identified, but both Beuermann et al. (2000), and Harrison et al. (2004) suggest that it must be brown dwarf-like object, and recent *Spitzer* observations detect strong mid-infrared emission that suggest this object is an L or T dwarf (Howell et al., 2006).

We have been monitoring EF Eri with regularity over the past 9 years, using its continued low state as an invitation from the binary to attempt to learn about its stellar components. During the Fall of 2004, we noticed that EF Eri, while becoming no brighter, began to show weak, narrow H α emission. The remainder of the Balmer series, and other spectral lines, are also now present. Detailed analysis of the H α emission line yields the first dynamical orbital velocity solution for EF Eri. We use this information and the remaining spectral features to determine the source of the emission and show that it is consistent with chromospheric activity on the sub-stellar secondary.

2. Observations

We present a number of observations in this paper from a variety of sources. The largest data set is from our monitoring program of EF Eri using the SMARTS telescopes at CTIO. These observations consist of multi-color photometry and optical spectroscopy covering the H α region. We also present a single blue spectrum obtained in Fall 2005 at the Apache Point Observatory and use it to compare EF Eri to the prototype polar, AM Her. The comparison reveals that both stars have white dwarfs with similar magnetic field strengths and both stars show stellar activity indicators during their low state. Finally, we present a high S/N, low state optical spectrum from Keck II revealing the full panorama of on-going spectral activity in EF Eri.

2.1. SMARTS

Photometric and spectroscopic monitoring of EF Eri has been accomplished using the SMARTS¹ facilities at Cerro Tololo. This program has operated from Aug. 2003 to the present and all data were obtained by the SMARTS service observers.

2.1.1. Photometry

The optical images were obtained using the ANDICAM dual channel imager on the SMARTS 1.3m telescope. ANDICAM obtains simultaneous optical and near-IR images, although EF Eri is too faint in its low state for us to make use of the near-IR capability. The optical detector is a Fairchild 447 2048x2048 CCD. We obtained 100 second integrations through the B, V, and I filters. The images are processed (overscan subtraction and flat-fielding) prior to distribution to SMARTS observers. Because we obtained only single images through each filter each night, the noise is dominated, in some cases, by cosmic rays and hot pixels.

We obtained 90 sets of useful images between 22 August 2003 and 21 December 2005. On 2 November 2005 UT we obtained continuous coverage of 1.09 orbital cycles in 36 V-band images between 2.34 and 3.81 hours UT (see §2.1.2).

We measured the star’s brightness using differential photometry with a 4'' radius aperture. The photometry is differential with respect to 5 nearby stars. One of these stars appears to a long term variable that has faded by about 0.06 mag in *B* and *V*, and 0.3 mag in *I* over our 850 day baseline. This object has been removed as a valid comparison star. The internal consistency of the remaining four comparison stars is <5 mmag. Uncertainties in the magnitudes of the target are dominated by counting statistics.

Figure 1a shows the SMARTS differential photometry in the *B*, *V*, and *I* bands for EF Eri spanning the last few years. We can use the SMARTS comparison stars and our previous calibrated observations of the EF Eri field (Harrison et al. 2003) to say that EF Eri has been amazingly constant in the optical during this time period; EF Eri has remained in the low state with $V \sim B \sim 18.2$ and $I \sim 17.8$. As an additional check on the state of EF Eri, we examined new K band images on 2005 July 30 UT kindly taken at the United Kingdom Infrared Telescope (UKIRT) and provided by S. Leggett and T. Geballe. Upon reduction,

¹SMARTS, the Small and Medium Aperture Research Telescope Facility, is a consortium of universities and research institutions that operate the small telescopes at Cerro Tololo under contract with AURA.

these images showed EF Eri to have a K magnitude of 15.2 ± 0.2 , the same value it has had for the past 8 years.

Figure 1b phases the Fig. 1a observations on the EF Eri orbital period of 81 min and our new spectroscopic ephemeris discussed below. The sine-like shape of the B light curve, with semi-amplitude near 0.1 mag, is similar to, but less well defined than in V and appears to be absent altogether in I . These light curve features show the same level, shape, and phasing as light curves presented in Harrison et al. (2003; their Fig. 2 shows observations obtained in 2001 Dec. ²). Similar to the Harrison et al. interpretation, we believe the weak blue photometric modulation is due to a surface feature on the white dwarf. We will discuss below (§3.3) whether this feature is consistent with a bright, warm region or a cool, higher opacity region near one of the accretion poles.

2.1.2. Spectroscopy

Our first two SMARTS spectra of EF Eri were obtained on 2004 Aug 13 UT and on 2004 Oct 19 UT. The two spectra look nearly identical and the second one is presented in Fig. 2. These spectra were obtained with the 1.5m SMARTS telescope using grating 13 providing 17\AA spectral resolution and covering most of the optical (3200\AA - 9500\AA). We note in Fig. 2 (as well as in the 13 Aug observation) the clear signature of the first two Balmer lines in emission ($H\alpha$ eq. width is -19\AA see §3.3), He I emission at 5876\AA , and the probable detection of the underlying Zeeman split absorption lines from the magnetic white dwarf.

Given our detection of Balmer emission, we continued monitoring EF Eri ultimately obtaining 10 sets of spectra with the RC spectrograph on the 1.5m SMARTS telescope starting on 20 Oct 2004 UT. (see Table 1). The RC spectrograph is a slit spectrograph with a $300''$ long slit oriented E-W and a Loral 1200×800 CCD detector. We made all our observations through a $110\mu\text{m}$ ($1.5''$) slit. EF Eri has a nearby unrelated companion star approximately $22''$ west-southwest. In order to orient the SMARTS observers with our field and to make completely sure we did not intersperse or include spectra of this nearby object, we purposefully obtained a spectrum of this star. This companion star appears to be a weak-lined, late-type star ($\sim K$) and has absolutely no spectral similarities to EF Eri: no emission lines, is significantly brighter³, and is easily avoided in the spectrograph slit.

²Note, Harrison et al. phased their light curves on the original Bailey photometric ephemeris.

³Note that in the familiar finding chart for EF Eri available from the Downes CV Atlas at <http://archive.stsci.edu/prepds/cvcat/> and other places, the nearby companion star and EF Eri appear similar in brightness. This image was obtained at a time when EF Eri was in a high (bright) state near

We obtained at least three spectral images at each epoch in order to filter cosmic rays. The basic spectral reductions subtract the overscan and divide each image by the normalized flat field image using a pipeline written in IDL. The spectrum in Figure 2 has 17 Å resolution and covers the entire optical spectrum out to 9300Å. All subsequent spectra were obtained with grating 47 in first order, with a wavelength range of 5652-6972Å and a resolution of 3.1Å. Wavelength calibration utilizes a Neon lamp exposure, taken at the start of the observing sequence. Exposure times for the individual frames range from 500 to 1200 seconds. We generated a median image from all the images at each of the 10 epochs. As these longer exposure times caused the spectral signal to be integrated over a significant fraction of the 81 minute orbital period, any radial velocity or line profile information, is smeared in the summed images.

EF Eri is a challenging target for spectroscopic work at a 1.5-m telescope. The SMARTS service observers are quite skilled and highly proficient and performed the spectral observations with great care. The SMARTS spectra of EF Eri on all occasions presents a weak (pseudo)continuum, with a typical S/N per pixel in the continuum <3. We extract the spectra from the images in two ways. First, we use a boxcar extraction with an extraction width set by a fit to the cross section of the spectrum at chip center. The background is measured above and below the spectrum, and linearly interpolated to the position of the source spectrum. Secondly, we fit a Gaussian atop a flat background at each column in the chip. In both cases, the location of the spectrum (the trace) is determined from a bright star observed that night, and shifted to match the position of the target. The width of the spectrum as a function of wavelength is determined from the trace of the bright star. The extraction width is not allowed to vary in the Gaussian fits. The flux from the Gaussian extraction is the analytical integration of the Gaussian fit.

We observed a spectrophotometric standard, either Feige 110 or LTT 4364, each night in order to convert the counts spectrum to a flux spectrum. Due to seeing-related slit losses, we do not obtain absolute fluxes, but rather use the standards to recover the shape of the continuum.

We know that the Balmer emission produced by the high state accretion in EF Eri greatly declined after the start of its 1997 Jan. low state (Wheatley & Ramsey 1998; Beuermann et al. 2000). Spectra obtained in Nov. 2000 (Reinsch et al. 2004; Euchner et al. 2002) show very weak Balmer emission with only H α being above the continuum. By March 2001, the Balmer emission had disappeared altogether (Harrison et al. 2003⁴) and remained

V=14.

⁴In Fig. 4 of Harrison et al., the authors claim that the H β emission line has weakened. A reexamination

absent as late as Aug. 2002 (Harrison et al. 2004; Howell 2004). On 13 Aug 2004 UT, we noted the presence of Balmer and He emission in EF Eri and thus began our SMARTS monitoring efforts. Therefore, we can only state that the H I emission in EF Eri started sometime between 2002 Aug. and 2004 Aug.

While our spectra are too poor for continuum flux measurements, in nearly all of them, H α emission was clearly seen, and we could obtain a measurement of its line center and equivalent width. To accomplish this, we Fourier-smoothed the individual spectra (see Figure 4), and then fit the spectra between 6400 and 6700Å with the sum of a quadratic background and a Gaussian line. The S/N of the (pseudo)continuum in our data is far too low to reveal any photospheric features from the white dwarf. The H α emission line is generally narrow, but can be significantly velocity-smearred even in a ten minute integration. We use the best-fit position of the Gaussian for the radial velocity analysis. A simple centroid of the emission line gives comparable results. Figure 5 shows one of the trailed SMARTS spectra of the H α emission line in EF Eri. The plot illustrates the obvious sinusoidal motion of the H α emission line as well as its modulation with phase.

2.2. Apache Point Observatory

Optical spectroscopy of EF Eri and AM Her were obtained on 2005 November 6 UT using the Double Imaging Spectrograph⁵ on the Apache Point Observatory 3.5 m. We used the high resolution gratings with a 1.5 arc-second slit to deliver a dispersion of 0.6 Å/pix. The central wavelength of the blue spectrum was 4500 Å, covering the spectral range $\lambda\lambda$ 3865 – 5094 Å. The exposure times for both AM Her and EF Eri were 20 minutes each, this is one-fourth of the EF Eri orbital period. The exposures were started at 6:21:56.0 11/06/2005 UT (EF Eri) and 1:18:30.4 11/06/2005 UT (AM Her). Both AM Her and EF Eri were in a low state during this time (see Kafka et al. 2005, 2006).

Figure 6 presents our APO observations of EF Eri and AM Her. The spectrum of AM Her has been over-plotted at a flux level about ten times below its real value. In Fig. 6, we note that the spectrum of AM Her rises to the blue, while EF Eri drops, a consequence of the difference of the white dwarf temperatures in the two polars. Balmer, Ca II (H&K), and He I emission is seen in both systems and has been associated with the secondary star

of this spectrum with respect to the pure Zeeman absorption spectrum observed in 2002 as well as model fits such as in Reinsch et al. 2004, show that it is likely that no Balmer emission was present in the Harrison et al. spectrum.

⁵<http://www.apo.nmsu.edu/Instruments/DIS/Default.html>

in AM Her.

2.3. Keck

On January 03, 2006 UT a 10 minute, medium resolution spectrum of EF Eri was obtained with ESI (Sheinis et al. 2002) in echellette mode on the Keck II telescope. This setup provided a useful spectral coverage of 4000–10,000Å in 10 spectral orders with a constant dispersion of 11.4 km s^{-1} pixel $^{-1}$. A slit width of 1" aligned along the parallactic angle was used with a plate scale of 0.127–0.183" pixel $^{-1}$ providing a resolution of 3000 to 5000 across the optical spectrum, giving 1.6Å resolution at H α . Wavelength calibrations were accomplished using Hg-Ne-Xe and Cu-Ar lamps. The active flexure control on ESI minimizes drift in the wavelength calibration and/or any fringing that is crucial for clean sky subtraction. The spectrophotometric standard Feige 110 was used for flux calibration. The data were reduced using standard IRAF routines with additional custom analysis routines to properly correct for the large curvature, strong nonlinear photometric response, and small tilt of sky lines.

Figure 7 shows our high S/N Keck spectrum of EF Eri. The underlying white dwarf continuum is now revealed, presenting the Zeeman split Balmer absorptions from the white dwarf. Figure 7 also shows the presence of narrow emission lines of the entire Balmer series of hydrogen, the Pickering series of He I (4388, 4471, 4922?, 5876, 6678, and 7065 Å), Na I, and the Ca II triplet (8498, 8542, 8662 Å). No He II emission is observed. The continuum slope change seen near 8600Å, also noted by Beuermann et al. (2000), is not a contribution from the secondary but, as shown by Harrison et al. (2003, 2004), maybe due to a weak cyclotron hump feature consistent with the 13-14 MG magnetic field present in EF Eri (see §3.2). Our high S/N Keck spectrum and our low resolution SMARTS spectrum (Fig. 3) confirms our belief that the SMARTS radial velocity data samples only the top of the H α emission line sitting on a pseudo-continuum.

3. Analysis

3.1. Radial Velocity Solution

The SMARTS spectral observations can be discussed as two groups. The first group (group one) are data specifically obtained for radial velocity and orbital motion determination. They all have a uniform integration time and were collected over a short time period in 2005 Nov, 2005 Dec (two separate nights), and 2006 Feb. The remaining SMARTS spectra

(group two) consist of our monitoring observations obtained between 2004 Oct and 2005 Nov (See Table 1). The four datasets that form group one cover at least one orbital period each in a continuous manner. Group two consists of spectra usually taken in threes and obtained in the months of 2004 Oct & Nov and 2005 Jul, Sep, and Nov. These latter data have various integration times, from 500 to 1200 seconds, with half being 1200 seconds or 1/4 of the orbital period of EF Eri.

Bailey et al. (1982) obtained optical and near-IR high state photometry for EF Eri over the observing season in Fall 1979. Those authors noted that the optical and near-IR light curves were complex and did not agree in shape over the various wavelengths, but the infrared light curves showed, on most nights, a narrow dip feature that nicely repeated. The center of this narrow dip was used to set a photometric ephemeris for EF Eri whereby the dip was chosen to be phase 0. Bailey et al. discuss the various light curves and conclude that the narrow dip was most likely caused by the secondary eclipsing the gas stream as it traveled toward the white dwarf. It was thus assumed that Bailey’s photometric phase 0.0 was near the true spectroscopic phase 0.0. All work on EF Eri since the Bailey et al. paper has used this photometric ephemeris and phasing as no other was available.

We initially focused on the group one data set, 45 spectra in total, and phased them on the orbital period given by Bailey et al. (1982). Our $H\alpha$ line center velocity measurements are presented in Figure 8. Each continuous set of observations for the four nights are represented by a different color as described in the figure caption. While our formal error in the measurement of the $H\alpha$ line center is $\sim 1\text{\AA}$ for most of the measurements, the spectra containing weaker emission lines (near phase 0.0) are a bit worse. Thus, in fitting our orbital solution, we used conservative 1σ error bars of $\pm 1.5\text{\AA}$ for each of the radial velocity measurements. We then added in the group two SMARTS spectra and produced a new radial velocity solution. The inclusion of the additional points produced a very similar (within the formal errors) result to that obtained with the group one data alone. This consistent behavior providing confirmation that the $H\alpha$ emission has remained constant in velocity behavior over the entire time we have detected it. Figure 8 shows the additional velocity measurements as a separate color. The Bailey et al. photometric phases are given on the top axis in Fig. 8 to illustrate the relationship between the older photometric phase and our new dynamic spectroscopic phasing.

Our best fit sine curve solution to the $H\alpha$ emission line centers for all our spectra yields a normal CV spectroscopic *primary star red-to-blue* crossing ephemeris for EF Eri of

$$T_0 = HJD2453716.61108(5) + 0.05626586(80)E$$

where orbital phase 0.0 is the secondary’s inferior conjunction. We have assumed that the orbit is circular and the components make their respective red-to-blue crossings 180 degrees

apart in phase and have used the orbital period determined by Bailey et al. (1982). Our best fit to the $H\alpha$ measurements yields a K_2 of $269 \pm 18 \text{ km sec}^{-1}$ and $\gamma=115 \pm 15 \text{ km sec}^{-1}$. Spectroscopic phase 0.0 (0.5) is equal to Bailey et al. photometric phase 0.41 (0.91). Note that all other plots in the paper use our new spectroscopic orbital phasing derived above.

The large value for K_2 indicates that the emission is produced on, or near, the secondary given its large value. It would be impossible for the white dwarf in this binary to have such a large K amplitude. We will show below that this emission, as appears true for both AM Her and VV Pup during their low states, is not caused by irradiation. Given our new dynamic orbital solution, the suggestion that the narrow photometric dip feature used by Bailey et al. to define phase 0.0 is caused by some sort of gas stream eclipse by the secondary cannot be correct.

3.2. Zeeman Absorption Spectroscopy and Cyclotron Emission

The nearly identical Zeeman absorption structures from the white dwarfs in both AM Her and EF Eri are easily seen in Fig. 6. AM Her has a listed magnetic field strength of 12.5 MG (Bonnet-Bidaud et al. 2000) while EF Eri’s field strength has been estimated in various ways to be between 17-35 MG (Warner 1995; Reinsch et al. 2004). Using Fig. 2 in Harrison et al. (2004) and our Keck spectrum presented here (Fig. 7) we can measure the Zeeman split $\pm\sigma$ components in the $H\alpha$ line to determine the surface magnetic field strength in EF Eri. We find the $\pm\sigma$ components are split from the main component of $H\alpha$ by $28 \pm 1.4 \text{ \AA}$ in both the older spectrum and our new Keck observation. Using Eq. 10 in Wickramasinghe & Ferrio (2000) for the linear regime, this splitting yields a surface field strength of $13.8 \pm 1 \text{ MG}$ for the white dwarf in EF Eri. We can also match our Fig. 7 $H\beta$ profile in some detail to the model work presented in Fig. 2 of Euchner et al. (2005). Doing so, yields a best magnetic field estimate of 13-14 MG. A rough comparison of our $H\alpha$ and $H\beta$ $\pm\sigma$ profiles with the detailed modeling for single, highly magnetic white dwarfs presented in Euchner et al. (2005, 2006) shows that we can estimate the linear Zeeman surface field to about $\pm 1 \text{ MG}$, but can do no better with these data.

Using our new spectroscopic phasing for EF Eri, we note that the optical light curve (Fig. 2) shows an asymmetric hump-like modulation consistent with a slight brightening (0.1 mag) centered near phase 0.4. The amplitude of this hump increases toward the blue. Phase 0.4 is where we would expect to be viewing the magnetic white dwarf at near right angles to the magnetic poles, thereby suggesting the slight flux increase may be related to cyclotron emission. Even though EF Eri is in a low accretion state, it is not zero as cyclotron humps, consistent with a 13-14 MG field, are seen in infrared spectra (Harrison et al. 2005). The

low state light curve could also be interpreted as having a luminosity dip from 0.8 to 0.0. This phase is where we would expect to have a more or less direct view of the main accretion pole on the white dwarf and/or the back end of the secondary . Given that the amplitude of the light curve increases to the blue, a cooler secondary back end seems to be ruled out. Perhaps we are seeing a dark spot on the white dwarf near the main accretion pole due to a region of higher opacity caused by atmospheric metals migrating toward the magnetic pole an forming a metallic lake (as seen in the single white dwarf GD394, Dupuis et al. 2000). This idea, however, is difficult to reconcile given the high UV flux levels observed in EF Eri in recent GALEX observations (Szkody et al., 2006). Weak mass accretion appears to be a common behavior in low state polars (e.g., Pandel & Cordova 2004; Howell et al. 2005) and is likely due to connected magnetic field lines between the two stars allowing the secondary wind (flares, prominences, etc.) to be accreted onto the white dwarf (see below).

3.3. The Origin of the Optical Emission Lines

It is useful to compare the current spectrum of EF Eri to the low state spectra of AM Her and VV Pup. All three show emission from H I and Ca II. While He I emission is clearly seen in VV Pup (Mason et al. 2006) and AM Her (Kafka et al. 2006), it is only confidently detected in our Keck spectrum of EF Eri. AM Her ($P_{orb}=3$ hr, M4V secondary) has been in a low state much of the past two years and Kafka et al. (2005, 2006) attribute the low state Balmer emission observed in AM Her to stellar activity on the secondary star. Their claim is based on a detailed examination of the Balmer emission, particularly $H\alpha$, including its radial velocity amplitude, its narrowness, and the line strength behavior throughout the orbit. Their analysis eliminates irradiation as the dominant source for the Balmer emission seen in AM Her during the low state. VV Pup, ($P_{orb}=100$ min) with an M7V secondary star, has also been in a low state for much of the past few years and the origin of its emission line spectrum has also been attributed to stellar activity on the secondary star (Mason et al. 2006). Both AM Her and VV Pup seem to show secondary star emission features at all times during their recent low states. EF Eri’s secondary, however, appears to not have had line emission for the first $\sim 5-7$ years of its low state. If the onset of the emission lines in EF Eri corresponds to the start of a stellar activity cycle, as we believe, this event did not cause EF Eri to immediately go into a high state. The activity in AM Her and VV Pup also seems to be uncorrelated with their high/low states starting or stopping. Thus, there does not appear to be a simple one-to-one correspondence between start/stop of stellar activity and high/low state transition in polars.

Our radial velocity curve makes it clear that the $H\alpha$ emission in EF Eri comes from

the secondary, but its source and the source of the Balmer, Pickering, Na I, and Ca II H&K emission is an open question. Irradiation and stellar activity are the two obvious choices for the cause.

3.3.1. Irradiation or Stellar Activity?

While irradiation is seen in some close interacting binaries, we know of no process whereby the cool white dwarf in EF Eri could suddenly start irradiating the secondary without any evidence for a change in the accretion rate. We also note that AM Her and VV Pup in their recent low states show no indication of irradiation induced or enhanced Balmer or other emission, even given their hotter white dwarfs (see §4). However, Kafka et al. (2006) conclude that it is possible that some low level irradiation may be present in AM Her during the low state but it is difficult to disentangle it from the much stronger activity-induced emission.

The presence of Balmer, Na I, Ca II (H&K and the IR triplet), and He I emission are all the usual signatures of stellar activity (Giampapa et al. 1978) as these lines form in the high photosphere / low chromosphere of the stellar atmosphere (see Vernazza et al. 1973). It has always been suspected that the secondary stars in CVs should be highly active, as they are rapidly rotating. However, there is little direct observational evidence of this assumption except in the polars during low states (e.g., Schwöpe et al. 2001).

Figure 9 presents the equivalent width (EW) of the H α line from our group one SMARTS spectra phased on the orbital period. We present the data for each night using a different color, the same scheme as in Fig. 8. If the H α line were produced by irradiation, we would expect the EW to be a strongly peaked with a maximum near spectroscopic phase 0.5 (the white dwarf facing side of the secondary), a result inconsistent with the measurements. What we see in Fig. 9 instead, is a nearly constant EW value, albeit slightly variable, and a possibly reduced, but non-zero, line width near phase 0.0, the back side of the secondary. As in AM Her and VV Pup, we find that the emission, and probably the stellar activity processes, are generally concentrated toward the white dwarf facing side of the secondary. A stronger magnetic field on the white dwarf and/or the alignment of active regions on the secondary star with the magnetic field (Simon et al. 1980) may cause a stronger “front side” concentration of activity. In addition, a tidal coupling model presented in Rottler et al. (2002) as a cause of white dwarf facing activity concentration will certainly be active in polars (and all CVs) and may help, or be the primary cause, of a longitudinal enhancement.

The concentration of stellar activity and starspots on the secondary, at or near L1, has

been previously assumed in the literature. For example, Hessman et al. (2000) presented a model to explain the high /low state behavior in AM Her. They used the modulated mass transfer levels in this polar as an indicator of the amount of starspots needed near L1. They concluded that nearly one-half of the “L1 region” of the secondary star would have to be covered with spots during a high state. Furthermore, Hessman et al. determined that this “L1 area concentration” could only be possible if the spots were somehow forced to wander into the region, possibly by a cyclic α^2 - Ω dynamo⁶. While this extreme level of starspot coverage has not been observed in AM Her or other polars during a high state, it is easily hidden by the much higher accretion luminosity.

While the EW of the H α emission above the (pseudo)continuum is relatively constant over all phases for a given orbit of EF Eri, there is evidence for long term changes of up to a factor of 2. Figure 10 presents the long term variations in the H α emission line equivalent width. The EW values have been integrated over each set of observations, or at least half the orbital period, so should not be affected by motions of the line across the underlying white dwarf Zeeman split absorption. Assuming the white dwarf continuum is not varying, and there is no substantial accretion, the observed variations in H α must be intrinsic to the secondary, probably the typical variations of active regions and starspots as observed in single active stars.

3.3.2. *He I and Ca II Emission*

He I emission is a useful tool for the determination of the physical conditions in which it is produced. The He I line at 5876Å is a triplet while that at 6678 Å is a singlet. Three mechanisms populate these states: (1) recombination to an excited state after photo-ionization by a $\lambda < 504$ Å photons; (2) collisional excitation from the He I ground state; (3) excitation of the singlets only by resonance scattering. This latter option is easily eliminated here as we detect both singlets and triplets in emission. Following the discussion related to the active M star AD Leo (Giampapa et al. 1978; Schneeberger et al. 1979) it is shown that the I(5876Å)/I(6678Å) ratio can be as high as 45 in quiescent prominences in the Sun but is near 3.3 in active prominences. This latter value is near the ratio of the triplet to singlet statistical weights (3.0).

⁶Note that in CVs with orbital periods below the period gap, the secondary stars are believed to have internal structures (fully convective or brown dwarf-like, e.g., VV Pup and EF Eri respectively) which are not expected to operate the α^2 - Ω dynamo in the same manner, or at all, compared with CV secondary stars above the period gap (e.g., AM Her).

The I(5876Å)/I(6678Å) ratio of 45 has been explained (Heasley et al. 1974) as a natural consequence of a typical quiet photosphere in a solar-like star. At cool temperatures (< 8000K) the He I resonance line photons, which populate the singlet levels, can not penetrate as far as the $\lambda < 504 \text{ \AA}$ photons which populate the triplet levels. As the temperature increases, i.e., moving into an active stellar atmosphere, the I(5876Å)/I(6678Å) ratio gets quickly reduced, almost independent of density, as collisional excitation from the ground state and collisional coupling of the triplet-singlet levels bring the two populations into closer accord. During low states, polars are not strong X-ray sources and even in high states, the X-ray emission is primarily produced at the white dwarf magnetic pole accretion region(s). We can conclude that the excitation of the secondary He I lines, during a low state, is not likely to be due to a strong $< 504 \text{ \AA}$ continuum as needed for option (1) above. Further evidence of the lack of X-ray induced lines is provided by the absence of He II or other high excitation emission lines in the optical spectra. Using the EF Eri spectra presented in Fig. 7, we can measure the I(5876Å)/I(6678Å) line ratio⁷. We find I(5876Å)/I(6678Å) = 3.7, a value expected for He I emission by collisional excitation in chromospheres hotter than 8000K. Athay (1965) provides rough guidelines for this sort of line emitting region yielding column densities of $\sim 10^{18} \text{ cm}^{-2}$ at temperatures of 20,000K or hotter.

The Ca II IR triplet, in emission in EF Eri, has peak fluxes in the ratio 1:2.6:2 for the 8498, 8592, and 8662Å lines, respectively. This is comparable to the flux ratio observed in a wide variety of objects from CVs (Persson 1988) to pre-main sequence stars (Hamann & Persson 1992) to active chromospheres in dMe stars (Pettersen 1989). The lines in the CVs are fairly broad, exhibit disk profiles, and form in the accretion disks; any weaker, narrower secondary emission being hidden. The dMe stars show narrow emission reversals in their Ca II photospheric absorption lines. The pre-main sequence stars show both broad and narrow components. The broad component seems to arise in a turbulent region near the base of the wind, while the narrow component is at rest with respect to the star, and may form in the chromosphere. In EF Eri the triplet lines are broadened by about 150 km/s, which is somewhat larger than, but comparable to, the expected $\sim 100 \text{ km/s } v \sin i$ of the secondary. We suspect an origin in the chromosphere of the secondary.

Given the above discussion, we conclude the most likely source of the line emission detected from the secondary in EF Eri is due to stellar activity. We have observed that in EF Eri, compared with AM Her and VV Pup, there was no secondary emission lines during the first 5-7 or so years of the low state but the emission began during the extended low state and has been present for the past 1.5 years. This discovery argues for the fact that we

⁷We can easily separate out the weaker Na emission sitting near the He 5876Å line.

have observed the onset of a stellar activity cycle in the sub-stellar companion star in EF Eri.

3.4. The Component Masses

The white dwarf in EF Eri has been observed during the current low state by a few observers (e.g., Beuermann et al. 2000, Howell 2004) who found it to be cool, near 9500K, and each made some attempt to determine its mass. Beuermann et al. (2000) provided the most rigorous determination for the mass of the white dwarf and concluded that the most likely value is near $0.6M_{\odot}$. This value, equal to the mean mass for white dwarfs found in CVs, has been generally used by the community for EF Eri. Harrison et al. (2002) fit optical and IR photometry of EF Eri in the low state and found that an $0.6M_{\odot}$ white dwarf worked quite well in the overall spectral energy distribution for EF Eri and led to an estimated distance of 90 pc, a value in agreement with the determination by Beuermann et al.

A recent paper by Wickramasinghe and Ferrario (2005) as well as former works by Liebert et al. (2003) and Liebert (1988) has shown that the masses for isolated magnetic white dwarfs are, on average, higher than non-magnetic white dwarfs. The mean masses of the two groups are $0.93M_{\odot}$ and $0.57M_{\odot}$ respectively. However, in cataclysmic variables the mean white dwarf mass seems to be near $0.6M_{\odot}$ regardless of magnetic or non-magnetic Warner (1995). Shylaja (2004) presents a compilation of derived masses for the white dwarfs in magnetic CVs and finds a trend toward higher mass (avg. near $0.85 M_{\odot}$) but lower mass magnetic white dwarfs ($0.4\text{-}0.6 M_{\odot}$) constitute about 1/4 of the sample. For now, we will adopt the value of $0.6M_{\odot}$ for the mass of the magnetic white dwarf in EF Eri but examine the consequences of it having a higher mass later on.

Using the relationship between the size of the secondary star Roche lobe and the binary mass ratio $q(=M_2/M_1)$ and assuming the secondary object, regardless of its true nature, is centrally condensed, we have

$$R_2/a = 0.462(q/(1 + q))$$

(Paczynski 1971; Huber et al. 1998). The secondary Roche lobe size (R_2) for EF Eri is $\sim 0.1R_{sun} \sim R_{Jupiter}$ or 7×10^7 meters (Howell et al. 2001) and the mean separation of the two stars, a , is 3.5×10^8 meters (Howell 2004)⁸. Substituting these values in the above equation yields a mass ratio of $q = 0.092$ for EF Eri. Taking the white dwarf mass to be $0.6M_{\odot}$, we

⁸Taking R_2 as equal to the Roche Lobe radius implies that the secondary star fills the Roche lobe. During a low state this may or may not be a valid assumption (see Howell et al. 2000; Howell 2005).

find $M_2=0.055M_\odot$. If the cutoff for core energy generation via hydrogen burning is taken as $0.06M_\odot$, then the secondary in EF Eri is sub-stellar and the binary may be a post-period minimum system (Howell et al. 2001). However, we should keep in mind the use of a “best guess” white dwarf mass and that our determined value for M_2 , within errors, is essentially at the stellar/sub-stellar mass boundary.

Taking the above masses at face value, our measured K_2 would predict a K_1 amplitude for the white dwarf of 25 km/sec, a value that will be extremely difficult to measure for the $V=18.5$ white dwarf in EF Eri, especially given that its Balmer absorption lines are Zeeman split and their relative location and shape will probably change throughout the orbit as the effective observed magnetic field strength changes. Of course, any precise K_1 measurement attempt could only be performed during a low state.

Beuermann et al. (2000) limited the secondary star in EF Eri to be later than M9 based on its non-detection in the red optical spectral region and Howell and Ciardi (2001) used a moderately good S/N K band spectrum to set a secondary mass limit of $\leq 0.05M_\odot$. Using their spectral energy distribution, Harrison et al. (2004) concluded that the secondary in EF Eri is near L5, a result that remained in agreement with the secondary’s continued non-detection in K band spectra (Harrison et al. 2005). Finally, Howell et al. (2006) have used Spitzer Space Telescope observations of EF Eri in the 3-8 micron region to further set a limit on the secondary finding that it is consistent with an object approximating a very late L or T type brown dwarf. All of these limits and mass estimates for the secondary in EF Eri seem to be in approximate agreement, generally independent of an assumed white dwarf mass. They all seem to indicate an M_2 value near $0.05-0.055M_\odot$. This mass for M_2 is also in agreement with the theoretical expectations for the secondary star in a CV such as EF Eri based on its orbital period and the assumption of the standard CV evolution model (Kolb & Baraffe, 1999; Howell et al. 2001; Politano 2004).

If the white dwarf in EF Eri has a higher mass, say as high as the average value for single magnetic white dwarfs, $0.95 M_\odot$, then M_2 would have a mass near $0.087M_\odot$ assuming q remains the same. While we cannot completely rule out this value for the mass of M_2 , such a star would not fit inside the secondary Roche Lobe if it were a normal main sequence object. Therefore, at this mass, we’d expect the secondary to be a dense He core with a thin hydrogen envelope, an object far less likely to show us what appears to be the typical signatures of an active chromosphere.

4. Discussion

4.1. Low States

Today, we know that most polars, including EF Eri, AM Her, and VV Pup have extended low states lasting years and that, in general, most polars show long term low states and/or spend much of their time in low states (Gerke et al. 2006 and refs therein). It is believed that all CVs (polars, dwarf novae, etc.) should have low states but that we only notice them in polars due to their lack of an accretion disk. In CVs with disks, if the mass transfer stops, the optical light may not show a significant dimming, as the optical light is dominated by or has a large contribution from the accretion disk. The stoppage of mass transfer in a non-magnetic CV may not be easily noted and if mass transfer restarts within a short time period ($\sim 2\text{-}4$ weeks), the entire event might escape detection. King and Cannizzo (1998) provide a theoretical framework for this idea and explore possible observational ramifications that could result. They conclude that current observations do not agree with their predictions of how a disk system would react to a stoppage of mass transfer. Given their work and the fact that polars often show extended low states it is hard to reconcile the idea that CVs with accretion disks (i.e., the non-magnetic white dwarf CVs) have low states similar to polars. The VY Scl stars may be the exception, as we discuss below.

It has been argued that the low states are a result of stellar activity cycles on the secondary star, in particular starspots migrating to the L1 region and stopping mass transfer for some period of time. The idea that “solar cycles” and starspots cause low states has been around for decades. Van Buren and Young (1985) suggested that changes in radius of the magnetically-active secondary in RS CVn systems drove the observed orbital period variations. The basic idea is that, during a stellar activity cycle, the magnetic pressure due to the enhanced subsurface magnetic fields displace gas, resulting in a fractionally larger stellar radius. The change in the moment of inertia drives the system out of synchronous rotation, and tidal torques then quickly bring the system back into synchrony. In the case of the RS CVn secondaries, the fractional change in the orbital periods ($\sim 10^{-6}$) requires a similar fractional change in the stellar radius. Applegate & Patterson (1987) applied this type of model to the cataclysmic variables, and predicted that there should be periodic $O-C$ variations on the magnetic activity period of the secondary. These magnetic activity periods are observed to be of order a decade long, within a factor of 2 of the length of the Solar cycle.

In the case of the polars, it may be this fractional change in the stellar radius that comes into play. Since the secondary is filling its Roche lobe when in the high state, a small reduction in the stellar radius as the magnetic activity wanes may lead to a cessation of

the accretion. The implication is that as the magnetic activity picks up, the star should then expand and eventually accretion should resume. This seems consistent with what we observed in the EF Eri secondary: the magnetic activity was at a minimum when the accretion ceased, and then increased prior to the start of the current high state.

The few direct observational results we do have that reveal stellar activity are all from polars in low states. We have seen that EF Eri entered a low state and its secondary was in-active, it turned on, and EF Eri stayed in a low state for another 1.5 years. On the other hand, AM Her and VV Pup with normal active M star secondaries, went into low states (recently, twice each) and from start to end during the low state the secondary was active, at a constant level, throughout. Single active M stars display spectroscopic activity indicators almost all the time but when they go into flaring or super-active episodes, their chromospheres can expand locally and eject material. This idea of active chromospheric expansion driving L1 mass loss was proposed by Howell et al. (2000) as the possible cause of high/low state. The model removed the need for a starspot at L1 but still kept the idea that stellar activity/flaring somehow triggers state changes. If some magnetic cycle connection is invoked to drive mass flows, then it may be that even in a high state, the photosphere need not fill its Roche lobe. The evidence for starspots at L1 and/or stellar activity *directly* starting and stopping high/low states seems not to exist.

Assuming, for the moment, that non-magnetic CVs do not undergo low states, can we explain such a phenomena? Polar secondaries have been shown to be normal main sequence stars (Harrison et al. 2005) while dwarf nova secondary stars, to date at least for systems above the period gap, have been shown to have spectra that reveal odd abundance patterns and are consistent with CNO processed material. Evidence has been presented that argues for a divergence in the evolutionary history of polars and non-magnetic CVs (see Schmidt et al. 2005; Harrison et al. 2005). If the secondaries in non-magnetic CVs are in fact remnant He cores from a past time when they were more massive, as has been suggested by Beuermann et al. (1998), Howell (2005), and Harrison et al. (2005), possibly evolving from Algols, then maybe normal stellar activity is not possible. If high/low states are somehow related to activity cycles on the mass donor, this idea may provide a natural explanation as to why dwarf novae and other non-magnetic CVs do not have polar-like low states.

Having said this, we must consider the VY Scl type of CV. These systems are believed to have non-magnetic white dwarfs and accretion disks, yet they show low state behavior that may be similar to that seen in polars. VY Scl stars have been used as “proof” of starspots and stellar activity but to date, this is more speculation than anything else. This sub-class of CV lies in the 3-4 hour period range, directly above the period gap. Howell et al. (2001) suggests these stars behave as they do because their secondaries are far from thermal

equilibrium and mass transfer can be highly modulated by thermal timescale changes caused by mass loss. If this is true or not, is yet to be seen, but observations of the secondary in VY Scl stars are likely to offer important clues as to the cause of high/low states.

4.2. Related Binaries

What does the secondary star do in terms of its activity cycles before, during, and after high/low state transitions? We have seen that stellar activity (as indicated by the usual optical emission lines) may be a constant feature in the normal M star secondaries of polars (i.e., VV Pup and AM Her) and that it can “turn on” during a low state (or at other times?) in at least one sub-stellar mass object, the secondary in EF Eri. Let us examine a few other binary systems in which magnetic fields and stellar activity play important roles. These objects may provide valuable clues toward our understanding of polars.

4.2.1. *RS CVn Binaries*

Low mass stars in close binaries exhibit enhanced activity, which is generally attributed to the amplification of the magnetic dynamo by tidally-enforced rapid rotation. The activity is generally saturated, with activity-related emission at the level of 10^{-2} to 10^{-3} of the bolometric flux. The secondaries of polars have similarly-rapid rotation and, if magnetic dynamo processes are present they may also be expected to exhibit activity at the saturated levels. However, the analogy is not exact, as the polar secondaries may have lost a significant fraction of their convective zones, with an effect on their ability to maintain or amplify a magnetic dynamo.

Stellar magnetic field emergence is known to be concentrated at certain active longitudes, both in the Sun and more active stars. The active RS CVn binaries are characterized by a “photometric wave”, interpreted as a spotted (and magnetically active) hemisphere that migrates around one of the stars with respect to the binary phase with a period of order a decade. The stars are tidally locked in such close binary systems; the migration is interpreted to represent differential rotation of the star, as the starspots migrate equator-ward as they do during a solar cycle. While there is evidence for such a photometric wave with a 6-9 month period in the pre-cataclysmic variable V471 Tau system (İbanoglu et al. 1994), there is also evidence that the chromospheric $H\alpha$ is enhanced near the substellar longitudes (Rottler et al. 2002). Because the strength of the emission decreased with time, Rottler et al. dismissed irradiation as the cause, and suggested that there is a permanent active longitude at the

substellar point, caused by tidal distortion of the convective dynamo. It is not clear whether this is in conflict with the observed wave migration (see §4.2.2).

There is spectroscopic evidence for enhanced flaring activity at the substellar longitudes in the RS CVn system UX Arietis (Simon, Linsky, & Schiffer 1980), and photometric evidence for enhanced flaring activity at the substellar longitudes in the close binary dMe system YY Gem (Doyle & Mathioudakis 1990). This is presumably attributable to recombination between the extended magnetic loops of the two stars, as in the models by Uchida and Sakurai (1985) (see Figure 11). There is no evidence addressing the long term variability of the flaring rates. If the recombination involves large-scale loops with sizes of order the binary separation, then flaring rates may remain more-or-less constant, but the rates may be enhanced when the active longitudes coincide with the substellar point.

Eclipse-mapping observations of RS CVn systems, of Algol, and of YY Gem have been brought to bear on the question of the presence of magnetic connections between stars, as might be expected if the substellar magnetic activity enhancement is indeed permanent. Preś, Siarkowski, & Sylwester (1995) and Siarkowski et al. (1996) modeled X-ray eclipse observations of the RS CVn systems TY Pyx and AR Lac, respectively. They concluded that in both cases a significant fraction of the emission arises between the stars, in magnetic loops connecting the stars. However, their unconstrained maximum entropy modeling solutions are not unique, and other equally good solutions without inter-stellar emission exist (see the review by Güdel [2004]).

4.2.2. *V471 Tau*

For V471 Tau, often used as the prototype pre-CV, the hot white dwarf ($T=35,000\text{K}$) was originally thought to irradiate the K secondary star. The evidence for this was $\text{H}\alpha$ emission from the secondary star which was observed to be concentrated toward the white dwarf with an equivalent width that peaked near orbital phase 0.5 and the emission line disappeared completely when looking at the back side of the secondary. However, multi-year observations of V471 Tau by Rottler et al. (1998, 2002) showed that in 1987, the $\text{H}\alpha$ emission was consistent with an irradiation interpretation while in 1990 the emission was much weaker and heavily concentrated toward the white dwarf and in 1992 the emission was completely absent. The (non-magnetic) white dwarf in V471 Tau was observed to be constant throughout this entire 5 year period showing that the secondary star emission was not due to irradiation by the hot white dwarf. Rottler et al. believe their observations are consistent with a “solar cycle”-like change that occurred in the K star.

Given their result with V471 Tau, Rottler et al. (2002) (re)examined a number of similar WD + RD systems all of which were supposed to show irradiation induced emission from the non-interacting secondary star. Of the ten hot white dwarf ($T=30,000$ to $60,000\text{K}$) plus red dwarf stars, only one (NN Ser, a WD+RD pair with $T_{WD}=55,000\text{K}$) is probably a true case of irradiation. The others are shown to have not enough UV flux to cause irradiation and the variable $H\alpha$ emission was consistent with activity induced emission lines. Using a model based on the number of $<912\text{\AA}$ photons available for irradiation of the secondary, they show that an incident UV flux at the surface of the secondary star of $\lesssim 1 \times 10^{10}$ ergs $\text{sec}^{-1} \text{cm}^{-2} \text{ster}^{-1}$ is not sufficient to produce irradiation induced emission lines. This value exceeds that present in EF Eri from its cooler but closer white dwarf ($F_{UV} \sim 1 \times 10^9$ ergs $\text{sec}^{-1} \text{cm}^{-2} \text{ster}^{-1}$) and, in fact, it exceeds nearly every CV when not in outburst.

4.2.3. *SDSS J121209.31+013627.7*

It is interesting to note here the discovery of an object that is very similar to EF Eri in the low state, SDSS J121209.31+013627.7 (Schmidt et al. 2005). These authors discuss this 90 minute, cool ($T \sim 10,000\text{K}$), orbitally synchronized magnetic (7-13 MG) white dwarf binary and present optical spectroscopy closely approximating those of EF Eri in a low state. They conclude, however, that SDSS J1212’s $H\alpha$ emission is most likely due to irradiation of the probable brown dwarf secondary based on a single epoch set of phase-resolved optical spectroscopy. The $H\alpha$ emission completely disappears when viewing the back end of the secondary star, a similar result to that observed once in V471 Tau. We therefore can ask, given the nearly similar nature of J1212 and EF Eri, if the secondary in J1212 is irradiated, why isn’t the secondary in EF Eri? With stellar activity seemingly being concentrated on the secondary at the sub-stellar point of the white dwarf, we will need to be careful in our observational interpretation of any detected emission from the secondary. Radiatively heated atmospheres (irradiation) and active stellar chromospheres (starspots etc.) may be hard to distinguish. If a star is irradiated, the apparent spectral type (photospheric temperature) should vary as the star rotates. Active chromospheres do fill in lines, which mimics an earlier spectral type in the K stars, but the veiling is wavelength-dependent. In M stars, the veiling might give a spectral type earlier than T_{eff} , since molecular band strengths are increasing with decreasing T_{eff} . Realistic, 3-D, magneto-hydrodynamic models of the secondary star and its magnetic, tidal, and radiative interaction with the primary are needed to fully understand the observations. J1212 and EF Eri are good starting points to use as proxies for our understanding of irradiation, stellar activity on brown dwarf-like secondary stars, and exoplanet physics. With no mass transfer currently underway in J1212, this system is an ideal candidate for multi-epoch observations to monitor and detail the nature

of the secondary star emission lines.

4.2.4. *Extra-Solar Planets*

The analogy between polars and the magnetically-active binary systems is imperfect. In none of these cases does the active star fill its Roche lobe, in none of these cases does the strength of the photospheric magnetic field exceed a few kG, and in none of these cases is the secondary star bathed in a strong external magnetic field. The tidal forces are also much stronger in EF Eri than even in V471 Tau, where the period is 8 times longer and the mass of the cool star is over an order of magnitude larger. A better analogy may be between a star and a planet.

Perhaps the answer to starting and stopping mass transfer lies in the area of magnetic (re)connection between the white dwarf and the secondary star. It was observed (Shkolnik et al. 2003) that for “hot Jupiter” type extra-solar planets, the host star Ca II H&K emission lines are sometimes modulated on the orbital period of the planet. A model proposed by Ip et al. (2004) explains this phenomenon as an interaction of the exoplanet magnetosphere with that of the parent star, in which a magnetic flux loop reconnects using the nearby planet as a conductor. In a polar, which has a much stronger field, it seems obvious that magnetic reconnection and closed field loops would have to pass through the secondary. This idea may also explain why the onset of stellar activity alone is not the direct cause of high/low states and why polars in low states seem to have a residual amount of mass transfer, probably magnetically connected secondary star wind accretion.

A possible observation of magnetic reconnection and closed field loops in the region near L1 but between the two stars (as illustrated in Fig. 11) was noted by Kafka et al. (2005, 2006) in their low state observations of stellar activity in AM Her. The $H\alpha$ emission line profile is triple peaked and leads to a model in which the regions on the secondary star where stellar activity occurs seem to be preferentially on the side facing the white dwarf and contain loop type structures surrounding the secondary. A similar white dwarf facing activity concentration and a similar multi-peaked $H\alpha$ line has been observed in V471 Tau (Young et al. 1991). The $H\alpha$ emission line satellites have been stable for over 2 years in AM Her and VV Pup showed a similar $H\alpha$ emission line structure during one of its recent low states (Mason et al. 2006).

4.3. Additional Observational Study

Stellar activity, as evidenced by emission lines such as H and Ca, is usually an optical bandpass specific proxy. Even very active stars, (see Fig. 12), show little obvious evidence for chromospheric activity in their near-IR and IR spectra. The reason that activity emission is so weak in the near-IR and IR bands is both a contrast effect and one of line formation. The activity induced emission lines in an active binary are often “filled in” by the emission from the bright photospheric continuum. Additionally, the typical spectral lines present in the IR region that one might expect to be in emission and associated with stellar activity (e.g., J - to K -band H I Paschen series and Ca lines) form too low in the stellar atmosphere to be greatly modulated or affected by an active chromosphere. In CVs, the contrast effect just mentioned can be provided by the high state accretion flux or accretion disk light, hiding not only the secondary but any possible activity-induced lines. Additionally, CV emission lines are generally very broad due to the high velocities in the disk or stream, again able to hide weaker, narrow lines caused by activity. Polars in low states offer the lack of additional (accretion) flux contribution allowing secondary star activity indicators to be observed in the optical. However, formation of the higher energy IR lines deeper in the stellar atmosphere still renders the 1-3 micron region a poor choice in the search for chromospheric activity. Indeed, near-IR spectroscopy of EF Eri obtained after the optical emission lines appeared (Johnson et al. 2005), show no sign of hydrogen or any other emission lines. ST LMi as well, was observed at 2.2 microns during a low state and no emission lines were seen, although Balmer emission was present (Howell et al. 2000). Thus, searches for stellar activity in CV secondaries are probably limited to low state observations in the optical, and as such, are mainly restricted to polars.

Low state observations, such as those presented herein, are generally difficult to gather as they require optical spectroscopy, often as target of opportunity observations, with fairly large telescopes, as low state polars tend to be faint. Phase resolved spectroscopy is required as the origin and cause of the spectral emission (or absorption, see Mason et al. 2006) features observed must be firmly determined. A single spectrum or even a single epoch of observations can easily confuse activity with irradiation. Polars are probably the easiest targets for this purpose as they show their high/low states directly while the VY Scl stars might be considered prime targets to go after as we know little about their low states or their secondary stars.

We have provided new direct spectroscopic evidence into the mix of understanding high/low states of polars and if and how these mass transfer changes are related to stellar activity. The simple idea of the turn on of stellar activity *directly* starting and stopping mass transfer (i.e., high and low states) seems ruled out as activity turned on in EF Eri,

yet it remained low for another 1.5 years, while stellar activity seems ever present in the secondary during low states of the polars AM Her and VV Pup. Just as we finish this paper, we can report that EF Eri has reentered a high state, reaching $V=15.6$ on 2006 March 04 (Stubbings, priv. comm.)⁹. Data obtained up to the time of this rebrightening (see Figs. 8, 9, 11) reveal no obvious change in the radial velocity, emission distribution on the secondary, or the EW of $H\alpha$ directly before the high state started. Our monitoring programs show EF Eri to be currently providing all its usual high state properties observed in the past, even after its nine year hiatus.

We want to make a special mention here of the undaunted observational effort of Rod Stubbings who, for over nine years, observed EF Eri and provided us with nothing, nothing to report that is, on EF Eri being visible until a few weeks ago when his email subject line “EF Eri brightened !!!” got the attention of astronomers the world over. Thanks Rod! We want to acknowledge Sandy Leggett & Tom Geballe for obtaining the K band images of EF Eri and UKIRT for its continued service observing program. Margeret Hanson kindly obtained the spectra of RS CVn for us. Frank Hill and Mark Giampapa have generously contributed their time to converse on and provide a great resource for information related to stellar activity on solar-like stars. We thank the referee for providing a number of useful comments. We are grateful for the support of Dean of Arts and Sciences J. Staros, Provost R. McGrath, and Vice President for Research G. Habich, all of Stony Brook University, for providing partial support that enabled Stony Brook’s participation in the SMARTS consortium. We thank the SMARTS service observers, J. Espinoza, D. Gonzalez, and A. Pasten, for taking the data, and for their dedication to the SMARTS effort. We thank C. Bailyn, the driving force behind the SMARTS consortium, for his leadership. This research was funded in part by NSF grant AST-0307454 to Stony Brook University. Some of the observations used herein were obtained at the W. M. Keck Observatory, which is operated as a scientific partnership among the California Institute of Technology, the University of California and the National Aeronautics and Space Administration, made possible by the generous financial support of the W. M. Keck Foundation. The authors wish to recognize and acknowledge the very significant cultural role and reverence that the summit of Mauna Kea has always had within the indigenous Hawaiian community. We are most fortunate to have the opportunity to conduct observations from this mountain. Part of this work was performed (M.E.H & R.H.B) under the auspices of the U.S. Department of Energy, National Nuclear Security Administration by the University of California, Lawrence Livermore National Laboratory

⁹Note that there seems to be nothing special about the location of the start of the high state (JD 2453798.) in Fig. 10.

under contract No. W-7405-Eng-48. We wish to thank the IAU for permission to reproduce Figure 10. Finally, SBH wishes to thank ESO headquarters in Chile for their support, and my host, Dr. E. Mason, for her coffee and cooking which provided a wonderful working environment, allowing the completion of this paper.

Table 1. SMARTS Spectroscopy Observing Log

HJD of Mid-exposure	Exp.Time (sec)	Spec. Phase ^a	H α Center (\AA)
2005 Nov 03 UT			
2453677.59576	600	0.5281550	6564.534
2453677.60287	600	0.6545194	6559.301
2453677.61000	600	0.7812392	6559.816
2453677.61709	600	0.9072481	6565.360
2453677.62420	600	0.0336125	6562.128
2453677.63843	600	0.2865190	6569.461
2453677.64047	600	0.3227754	6567.428
2453677.65265	600	0.5392477	6563.449
2453677.65976	600	0.6656121	6559.426
2453677.66685	600	0.7916210	6557.741
2453677.67396	600	0.9179854	6560.756
2005 Dec 12 UT			
2453716.57245	600	0.2517711	6568.204
2453716.57955	600	0.3779577	6568.298
2453716.58668	600	0.5406775	6564.490
2453716.60089	600	0.7572286	6558.563
2453716.60799	600	0.8834152	6566.133
2453716.61512	600	0.0101350	6566.893
2453716.62222	600	0.1363217	6567.989
2453716.62933	600	0.2626860	6569.877
2453716.63644	600	0.3890504	6571.038
2453716.64354	600	0.5152371	6565.521
2453716.65064	600	0.6414237	6559.827
2453716.65774	600	0.7676103	6558.431
2453716.66487	600	0.8940302	6562.807
2453716.67201	600	0.0212277	6570.044
2005 Dec 24 UT			
2453728.60122	600	0.0362933	6559.763
2453728.60833	600	0.1626577	6573.287
2453728.61544	600	0.2890221	6569.500

Table 1—Continued

HJD of Mid-exposure	Exp.Time (sec)	Spec. Phase ^a	H α Center (\AA)
2453728.62254	600	0.4152087	6567.619
2453728.62965	600	0.5415731	6563.255
2453728.63677	600	0.6681152	6557.919
2453728.64387	600	0.7943018	6558.931
2453728.65099	600	0.9208439	6563.869
2006 Feb 05 UT			
2453771.55291	600	0.4683228	6570.381
2453771.55975	600	0.5899048	6564.660
2453771.56685	600	0.7160645	6560.325
2453771.57396	600	0.8424683	6558.134
2453771.58106	600	0.9686279	6565.417
2453771.58817	600	0.0949707	6570.402
2453771.59530	600	0.2217407	6573.849
2453771.60241	600	0.3480835	6570.223
2453771.60950	600	0.4740601	6567.156
2453771.61661	600	0.6004639	6563.936
2453771.62374	600	0.7271729	6559.603
2453771.63084	600	0.8533325	6558.002
Other Measured Spectra			
2453298.61870	600	0.1806642	6570.467
2453298.62590	600	0.3085938	6569.269
2453298.63500	900	0.5014648	6564.754
2453330.57980	600	0.2177734	6571.960
2453330.58620	600	0.3315430	6569.405
2453579.89020	500	0.1430664	6570.897
2453579.89620	500	0.2497559	6571.325
2453579.90220	500	0.3564453	6569.764
2453620.72200	1200	0.9091797	6557.291
2453620.73610	1200	0.1597900	6569.510
2453620.75020	1200	0.4104004	6568.200
2453621.75480	1200	0.2648926	6569.407

Table 1—Continued

HJD of Mid-exposure	Exp.Time (sec)	Spec. Phase ^a	H α Center (\AA)
2453621.76890	1200	0.5155028	6566.310
2453621.78300	1200	0.7661133	6556.565
2453635.73010	1200	0.6446533	6562.242
2453689.63210	600	0.5705872	6563.307

^aDetermined using the new spectroscopic ephemeris given herein. Phase 0.0 equals the time of primary (white dwarf) red-to-blue crossing which equals the time of secondary inferior conjunction. Spectroscopic phase 0.0 = Bailey et al. photometric phase 0.41.

REFERENCES

- Applegate, J.H. 1992, ApJ, 385, 621
- Applegate, J.H., & Patterson, J. 1987, ApJL, 322, L99
- Athay, R. G., 1965, ApJ, 142, 755
- Bailey, J., Hough, J. H., Axon, D. J., et al., 1982, MNRAS, 199, 801
- Bianchini, A., 1992, ASOC, 29, 284
- Beuermann, K., Baraffe, I., Kolb, U., Weichhold, M., 1998, A&A, 339, 518
- Beuermann, K., Wheatley, P., Ramsay, G., Euchner, F., Gnsicke, B. T., 2000, A&A, 354, L49
- Charles, P., & Mason, K., 1979, ApJ, 232, L25
- Cooke, B., et al., 1978, MNRAS, 182, 489
- Doyle, J.G. & Mathioudakis, M. 1990, A&A 227, 130
- Dupuis, J., et al., ApJ, 2000, 537, 977
- Euchner, F., Reinsch, K., Jordan, S., Beuerman, K., & Gansicke, B., 2005, A&A, 442, 651
- Euchner, F., Jordan, S., Beuerman, K., Reinsch, K., & Gansicke, B., 2006, A&A, 451, 671
- Euchner, F., Jordan, S., Beuermann, K., Gansicke, B., & Hessman, F., 2002, A&A, 390, 633
- Gerke, J., et al, 2006, PASP, 118, 678
- Giampapa, M. S., Schneeberger, T. J.; Linsky, J. L.; Worden, S. P., 1978, ApJ, 226, 144
- Griffiths, R., et al., 1979, ApJ, 232, L27
- Güdel, M., 2004, A&ARv, 12, 71G
- Hamman, F. & Persson, S.E. 1992, ApJS, 82, 247
- Harrison, T. E., Howell, S. B., Szkody, P., Cordova, F. A., 2005, ApJ, 632L, 123
- Harrison, T. E., Osborne, H. L., Howell, S. B., 2005, AJ, 129, 2400
- Harrison, T. E., Howell, S. B., Szkody, P., et al., 2004, ApJ, 614, 947

- Harrison, T. E., et al., 2004, *AJ*, 127, 460
- Harrison, T. E., Osborne, H. L., Howell, S. B., 2004, *AJ*, 127, 3493
- Harrison, T. E., Howell, S. B., Huber, M. E., et al., 2003, *AJ*, 125, 2609
- Heasley, J., Mihalas, D., and Poland, A., 1974, *ApJ*, 192, 191
- Hessman, F., Gansicke, B., and Mattei, J., 2000, *A&A*, 361, 952
- Howell, S. B., et al., 2006, *AJ*, 131, 2216
- Howell, S. B., et al., 2006, *ApJ*, in press
- Howell, S. B., 2005, *ASPC*, 330, 67
- Howell, S. B., Harrison, T. E., & Szkody, P., 2004, *ApJ*, 602, L49
- Howell, S. B., 2004, *ASPC*, 315, 353
- Howell, S. B. & Ciardi, D. R., 2001, *ApJ*, 550, 57
- Howell, S. B., Nelson, L., & Rappaport, S., 2001, *ApJ*, 550, 518
- Howell, S. B., Ciardi, D. R., Dhillon, V. S., Skidmore, W., 2000, *ApJ*, 530, 904
- Huber, M. E., Howell, S. B., Ciardi, D. R., Fried, R., 1998, *PASP*, 110, 784
- İbanoglu, C., Keskin, V., Akan, M.C., Evren, S., & Tunca, Z. 1994, *A&A*, 281, 811
- Ip, W-H, Kopp, A, Hu, J-H., 2004, *ApJ*, 602L, 53I
- Johnson, J. J., Campbell, R. K., Harrison, T. E., Howell, S. B., 2005, *AAS*, 207, 7018
- Kafka, S., et al., 2006, *AJ*, in press
- Kafka, S., Honeycutt, R. K., Howell, S. B., Harrison, T. E., 2005, *AJ*, 130, 2852
- King, A. & Cannizzo, J., 1998, *ApJ*, 499, 348
- Kolb, U., & Baraffe, I., 1999, *MNRAS*, 309, 1034
- Liebert, J., Kirkpatrick, D., Cruz, K., et al., 2003, *ApJ*, 125, 343
- Liebert, J., Bergeron, P., Holberg, J. B., 2003, *AJ*, 125, 348
- Liebert, J., 1988, *PASP*, 100, 1302

- Mason, E., et al., 2006, A&A, submitted
- Paczynski, B., 1971, ARA&A, 9, 183
- Pandel, D., Cordova, F. A., 2005, ApJ, 620, 416
- Persson, S.E. 1989 PASP, 100, 710
- Pettersen, B.R. 1989, A&A 209, 279
- Politano, M., 2004, ApJ, 604, 817
- Preś, P., Siarkowski, M. & Sylwester, J. 1995, MNRAS, 275, 43
- Reinsch, K., Euchner, F., Beuermann, K., Jordan, S, 2004, ASPC, 315, 71
- Rottler, L., Batalha, C., Young, A., & Vogt, S., 1998, AAS, 192, 6720
- Rottler, L., Batalha, C., Young, A., & Vogt, S., 2002, A&A, 392, 535
- Siarkowski, M. et al., 1996, ApJ, 473, 470
- Schwope, A. D., Schwarz, R., Sirk, M., & Howell, S. B., 2001, A&A, 375, 419
- Schmidt, G. D., Szkody, P., Silvestri, N., 2005, ApJ, 630, L173
- Schmidt, G. D., Szkody, P., Vanlandingham, K. M., 2005, ApJ, 630, 1037
- Schneeberger, T. J., Linsky, J. L., McClintock, W., Worden, S. P., 1979, ApJ, 231, 148
- Sheinis, A., et al. 2002, PASP, 114, 851
- Shkolnik, E., Walker, G., & Bohlender, D., 2003, ApJ, 597, 1092
- Shylaja, B. S., 2004, ASPC, 315, 346
- Simon, T., Linsky, J., & Schiffer, F., 1980, ApJ, 239, 911
- Szkody, P., et al., 2006, ApJL, submitted
- Tapis, S., 1977, ApJ, 212, L125
- Uchida, Y., and Sakurai. T., 1985, IAUS, 107, 281
- Van Buren, D., & Young, A., 1985, ApJ, 295, L39
- Vernazza, J. E., Avrett, E. H., Loeser, Rudolf, 1973, ApJ, 184, 605

Walter, F.M., Beck, T., Morse, J., Wolk, S. 2003, AJ, 125, 2123

Walter, F., Gibson, D., and Basri, G., 1983, ApJ, 267, 665

Warner, B., 1995, “Cataclysmic Variable Stars”, Cambridge University Press

Wheatley, P., & Ramsay, G., 1998, ASPC, 137, 446

Wickramasinghe, D. T., Ferrario, L., 2000, PASP, 112, 873

Young, A., Rottler, L. & Skumanich, A., 1991, ApJ, 378, L25

Fig. 1.— 1a - EF Eri has remained stubbornly inactive during this 2.3 year interval as evidenced by the presented SMARTS photometry. The cluster of points at JD 3677 in the V band represents a 90 minute, full orbit campaign as discussed in the text. These differential magnitude light curves are plotted as usual, that is smaller numbers being brighter. The magnitude uncertainties are dominated by counting statistics in EF Eri. 1b - The differential photometry from 22 August 2003 through 21 December 2005, shown in Fig. 1a, folded on EF Eri's orbital period and new spectroscopic ephemeris as given in the text. The light curve half-amplitude is 0.09 and 0.08 mag in the B and V bands, respectively, with no significant modulation in the I band. This long term light curve is in good agreement with the single orbit light curve presented in Fig. 2 of Harrison et al. (2003), the latter being phased on the Bailey ephemeris. The differential light curves are plotted as usual, that is smaller numbers being brighter.

Fig. 2.— Our SMARTS spectrum of EF Eri obtained on 19 Oct 2004 UT. The Balmer and other emission lines are obvious as well as the underlying Zeeman split absorption lines due to the white dwarf. The emission lines appear to be weaker than those observed in Jan 2006 (see Fig. 7), but the spectral resolution is 17\AA , so the lines may simply be weaker relative to the continuum. The spectrum is flux calibrated and presented in arbitrary units.

Fig. 3.— The radial velocity of the $H\alpha$ emission line and the simultaneous V -band photometry from SMARTS on 3 November 2005. The radial velocities are from a Gaussian fit of the emission feature; the uncertainties represent a $\pm 1\text{\AA}$ systematic uncertainty due to velocity smearing and the skewing due to a non-flat underlying continuum. This shows the relation between the photometric orbital modulation of the white dwarf and the orbital location of the secondary.

Fig. 4.— Representative SMARTS spectra of EF Eri. The top three spectra are single 10-minute exposures while the bottom spectrum (thick line) is their sum. The vertical dotted line represents the rest velocity of H-alpha. Fluxes for each spectrum are on the same scale, but are offset by one unit from the previous spectrum. Compare these observations with the Keck spectrum of EF Eri (Fig. 9) and you'll see that the SMARTS data allows us to measure the top of the $H\alpha$ profile.

Fig. 5.— A trailed spectrum of EF Eri for the observations obtained on 4 Feb 2006. The slightly jumpy nature of the $H\alpha$ emission line is mainly due to limited phase sampling of the ultra-short 81 minute binary orbit. Changes in the line strength are due to small seeing variations but also have a real component as discussed in the text (See Fig. 9). The data are not smoothed and the bright spot near phase 0.8 at $\sim 6700\text{\AA}$ is a cosmic ray.

Fig. 6.— A comparison of the low state blue spectra of AM Her and EF Eri. These polars

have white dwarfs with similar magnetic field strengths (near 13 MG) but different white dwarf temperatures (20,000K for AM Her, 9500K for EF Eri). Their orbital periods are different as well, 3 hours vs. 81 minutes. Note the presence in both stars of Ca II H&K emission as well as how similar the Zeeman split white dwarf Balmer lines are. These spectra were obtained in Oct. 2005 at the 3.5-m APO telescope and had integration times of 20 minutes each, a value that is one-third of EF Eri’s orbital period ($P_{\text{orb}} = 81 \text{ min}$). The ordinate axis is correct for AM Her, while EF Eri has been multiplied by ten.

Fig. 7.— EF Eri as observed by Keck II in Jan 2006. The spectrum covers the majority of the optical band pass at quite good S/N (full range shown at top left) and reveals the set of emission lines from the secondary (see expanded views). The underlying white dwarf Balmer absorption lines are Zeeman split and reveal the surface magnetic field strength. See text for details.

Fig. 8.— The $H\alpha$ radial velocity curve for EF Eri based on SMARTS spectroscopy. The solid line is our best fit as described in the text. The top axis shows the photometric phase as determined by Bailey et al. (1982) and the bottom axis show our new spectroscopic orbital phase as described in the text. Each of the group one nights are shown in a different color: Red = 2005 Nov 03, Green = 2005 Dec 12, Blue = 2005 Dec 24, Orange = 2006 Feb 05. The purple points show our remaining monitoring RV measurements (see Table 1). See the text for details.

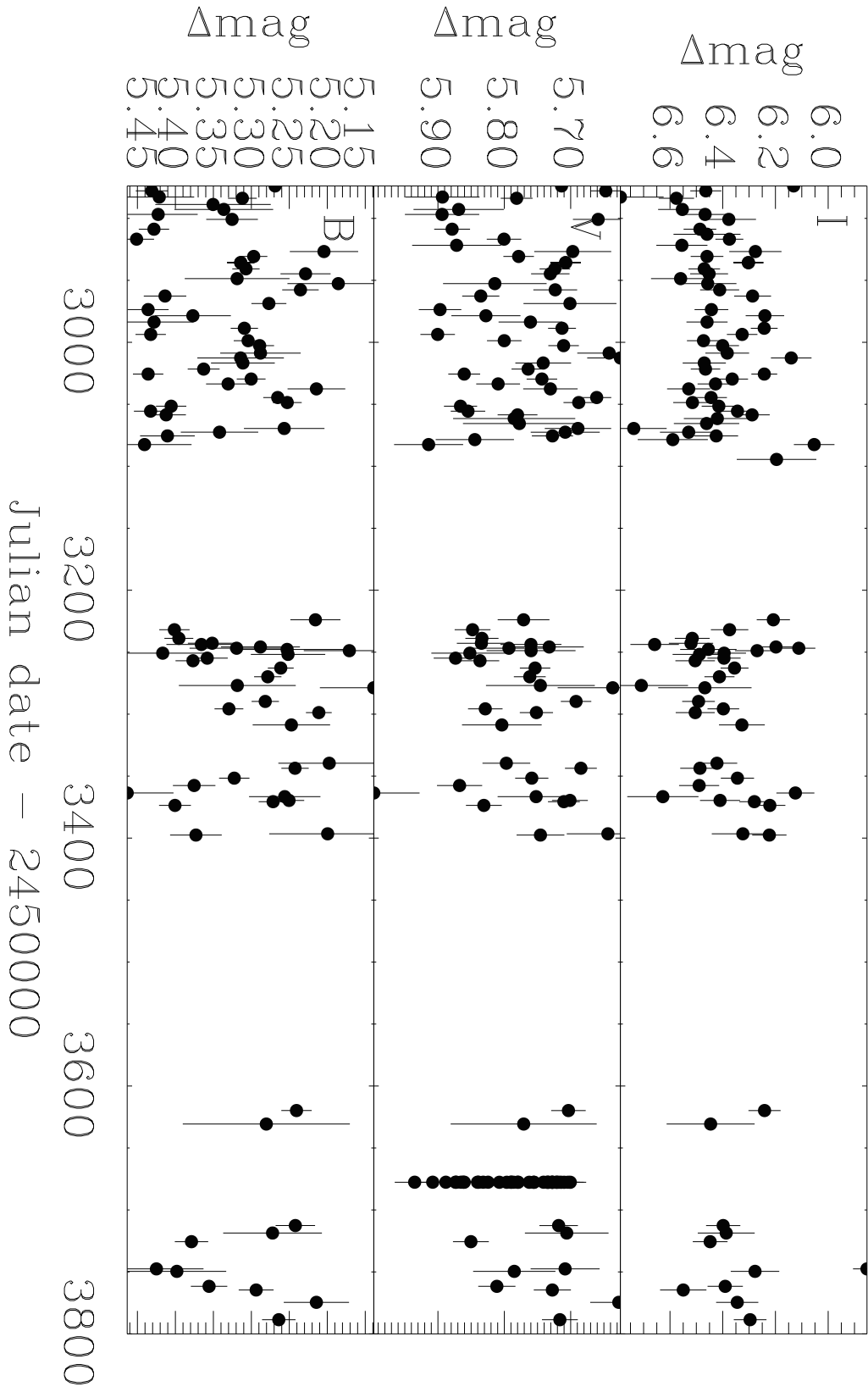
Fig. 9.— The phase resolved equivalent width of the $H\alpha$ emission line for the four group one nights in Nov. and Dec. 2005 and Feb 2006. Each orbit is shown by a different color (and symbol; 2005 Nov 03 is a filled square, 2005 Dec 12 is a filled star, 2005 Dec 24 is a filled triangle, and 2006 Feb 05 is a filled circle) following the scheme used in Fig. 8. The data are phased on the spectroscopic ephemeris presented in the text and each measurement has an approximate uncertainty of $\pm 2\text{\AA}$. The eq. width of the line is essentially constant at all phases with a possibly weaker line during phases 0.9 to 0.1, the back side of the secondary.

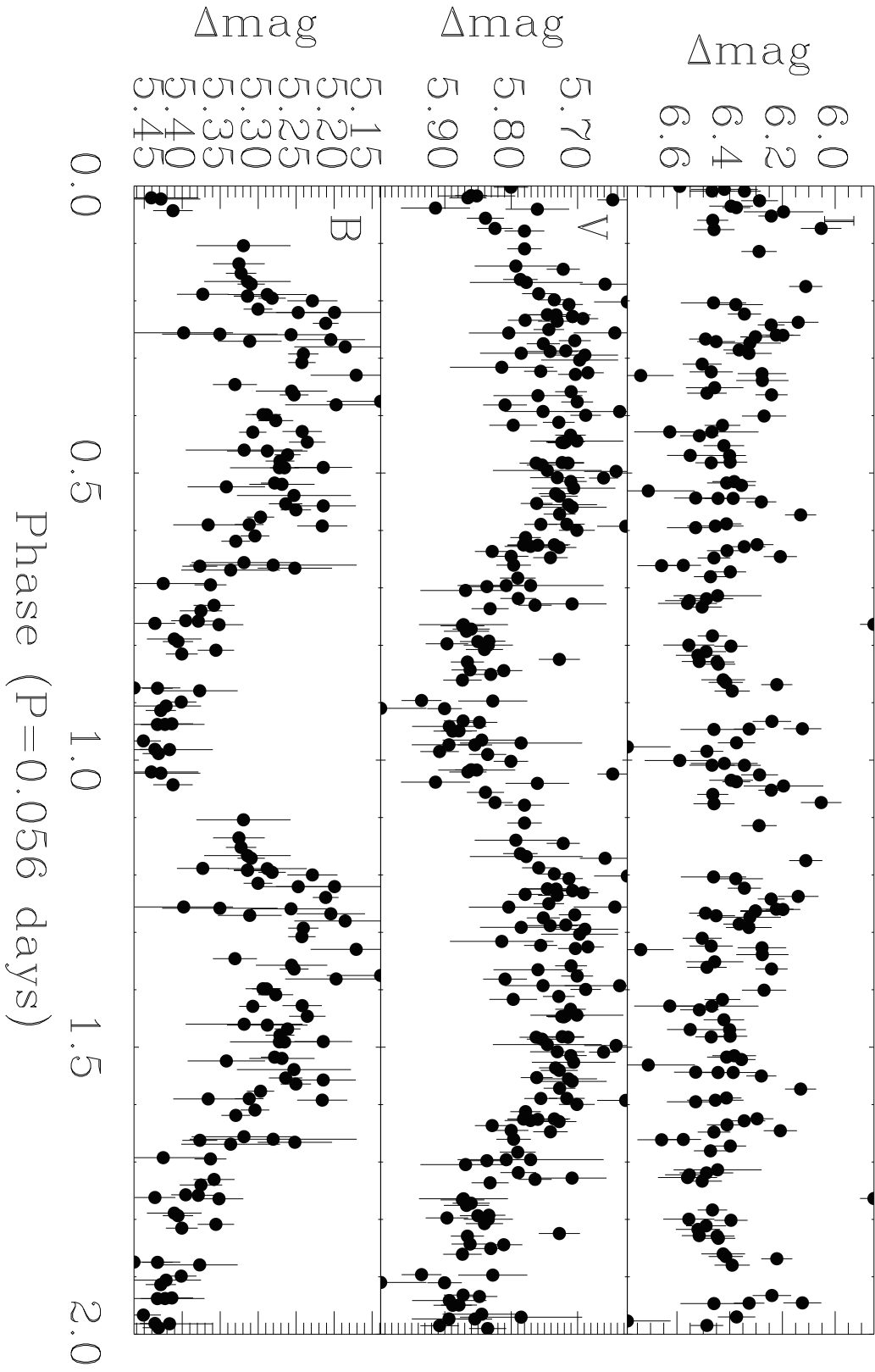
Fig. 10.— The long term variation of the $H\alpha$ equivalent width integrated over the full observation (0.4 - 1.2 orbital cycles). The equivalent width is plotted (i.e., the line is in emission) and the units of W_λ are \AA .

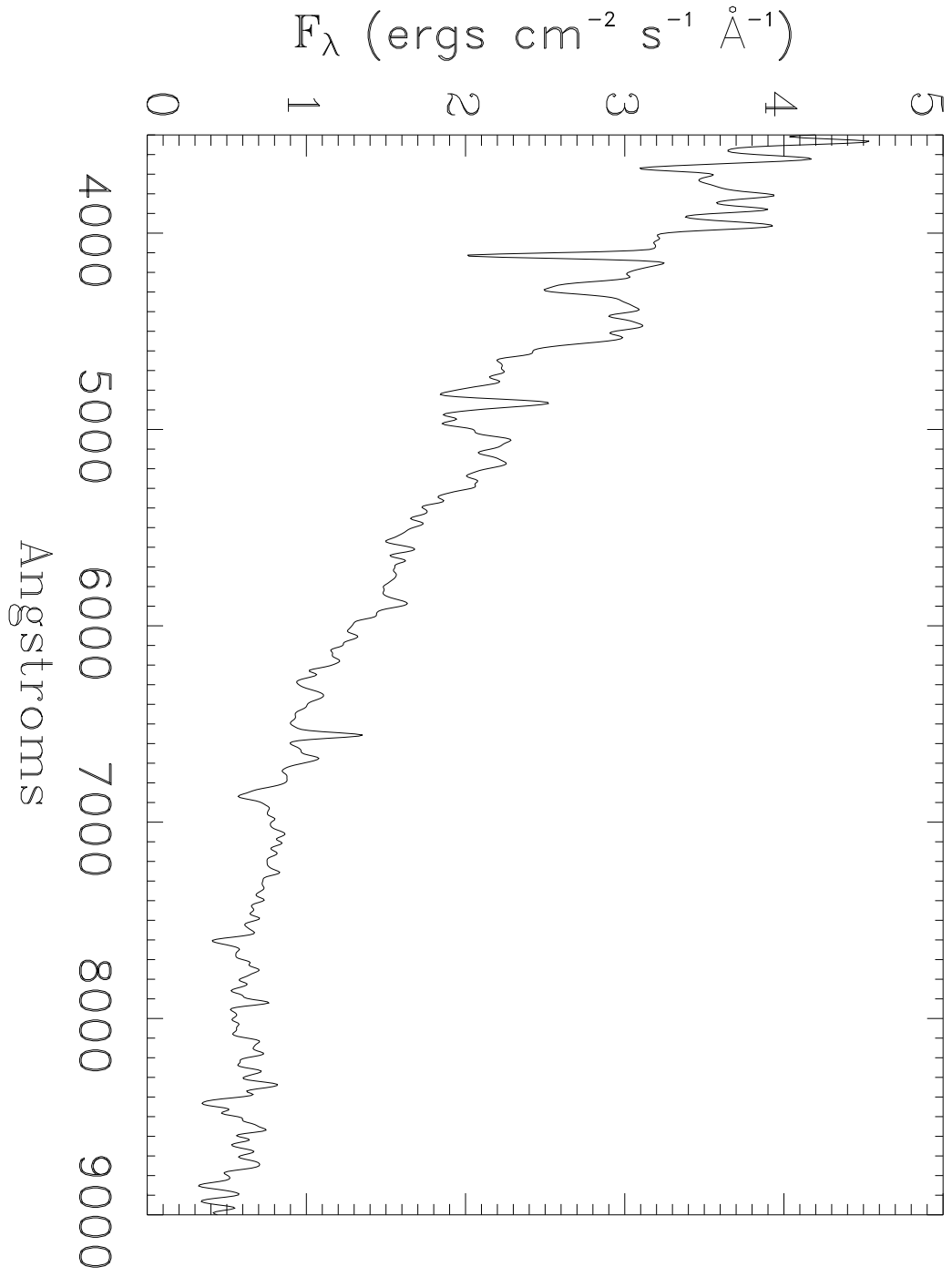
Fig. 11.— Magneto-dynamical model of the magnetic field interactions between the two component stars in an RS CVn binary. RS CVn stars are highly chromospheric active binaries often containing a KIII (top star here) having a polar magnetic field near 1000G and a main sequence F-G star having a polar field of $\sim 100\text{G}$. The stars orbit in a few to tens of days and have their rotation locked to the orbit. Changes in the magnetic field structures, due to starspot migration via differential rotation, causes flux tube connection, breaking,

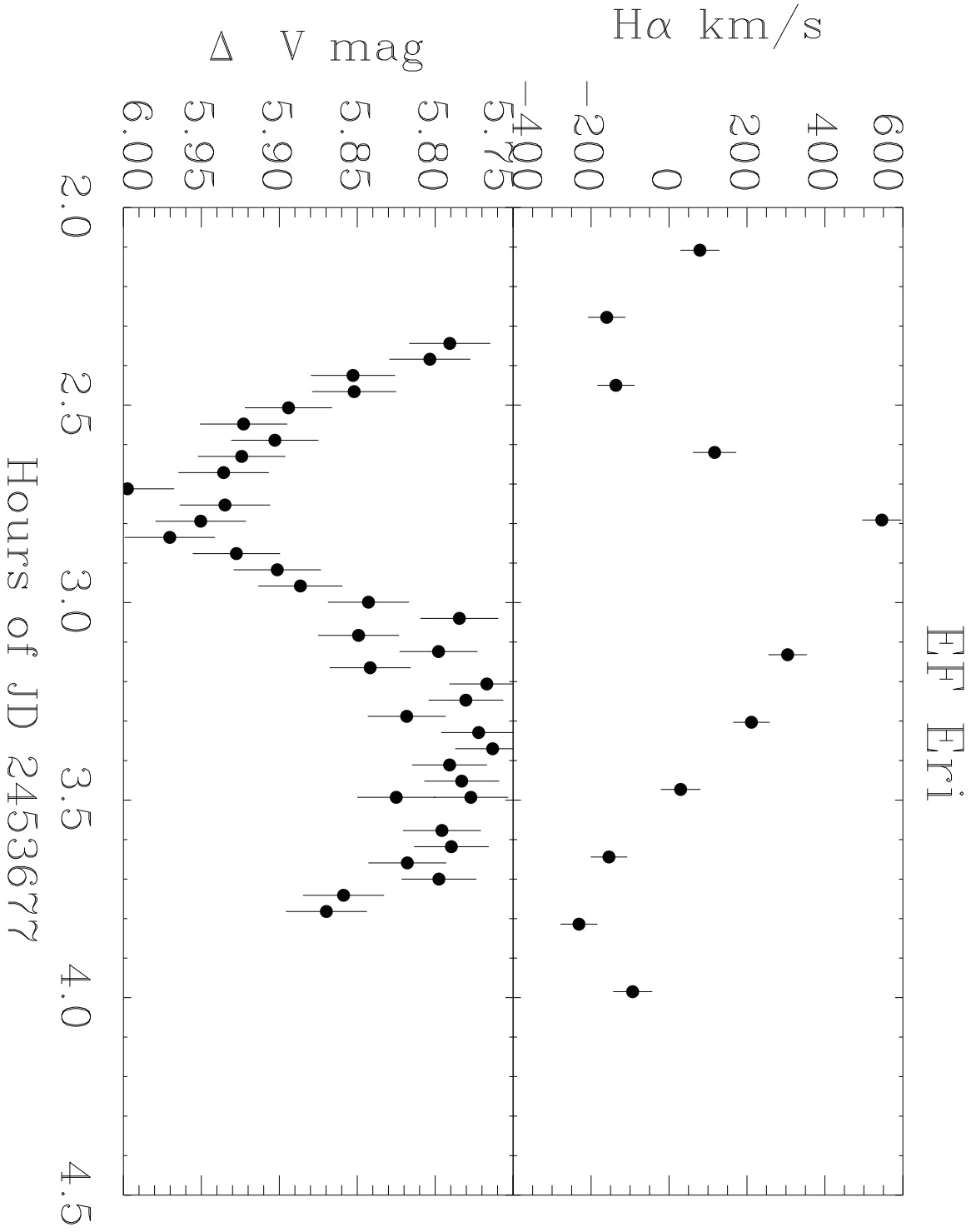
and reconnection events. Direct magnetic pole to starspot field lines exist and the majority of the chromospheric activity in the K star occurs on the companion facing hemisphere. One can imagine a similar but greatly enhanced process might occur in polars with the secondary star activity concentrated toward the white dwarf. Figure reproduced with permission from Y. Uchida and T. Sakurai, "Magnetodynamical Processes in Interacting Magnetospheres of RS CVn Binaries", published in IAU Symposium Series n. 107 "Unstable Current Systems and Plasma Instabilities in Astrophysics", pp. 281-285, 1985, D. Reidel Publishing Co.

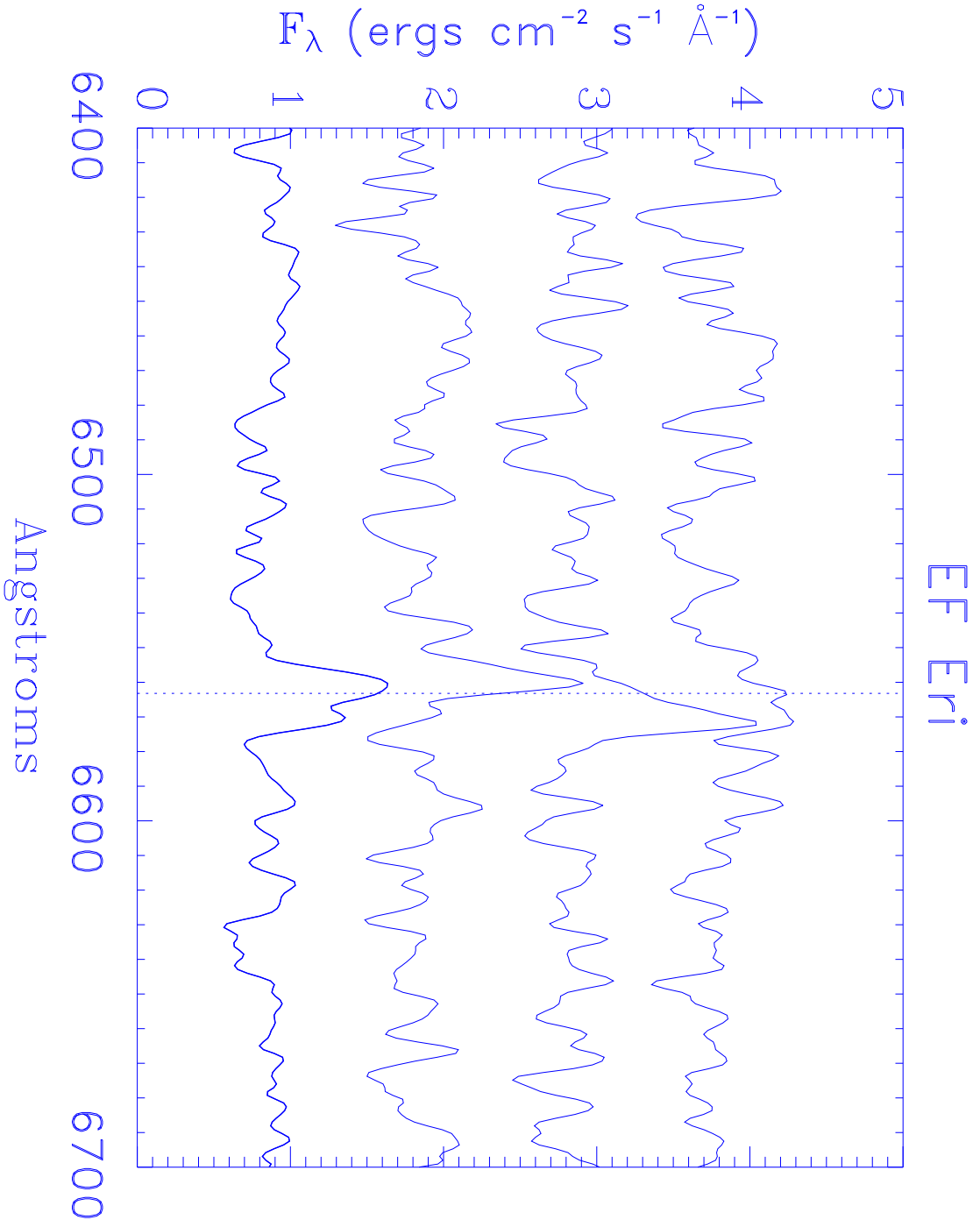
Fig. 12.— IRTF SPEX spectra of the highly active stars (a) RS CVn and (b) HD28867S. RS CVn, a short period active binary system, presents an example of a contrast issue as the giant companion's photosphere fills in the activity induced emission in the near-IR (i.e., Ca II triplet) but we do observe a weak He 10830Å emission line. In HD28867S, an M2 pre-main sequence star (Walter et al. 2003), we again see a He 10830Å emission line, but with a P Cygni profile. The emission is at zero velocity; the absorption is likely due to accretion in this young star. H I Paschen γ is weakly in emission, with an equivalent width of -0.4Å. The Ca II IR triplet is in absorption. While both stars show strong Ca II H&K and H α emission in the optical, their infrared spectra do not contain a similar wealth of strong emission lines generated by stellar magnetic activity at temperatures of 6000-20000K. This is due both to contrast against a bright photosphere near the peak of the Planck function, and the depth of the IR line formation in stellar atmospheres.

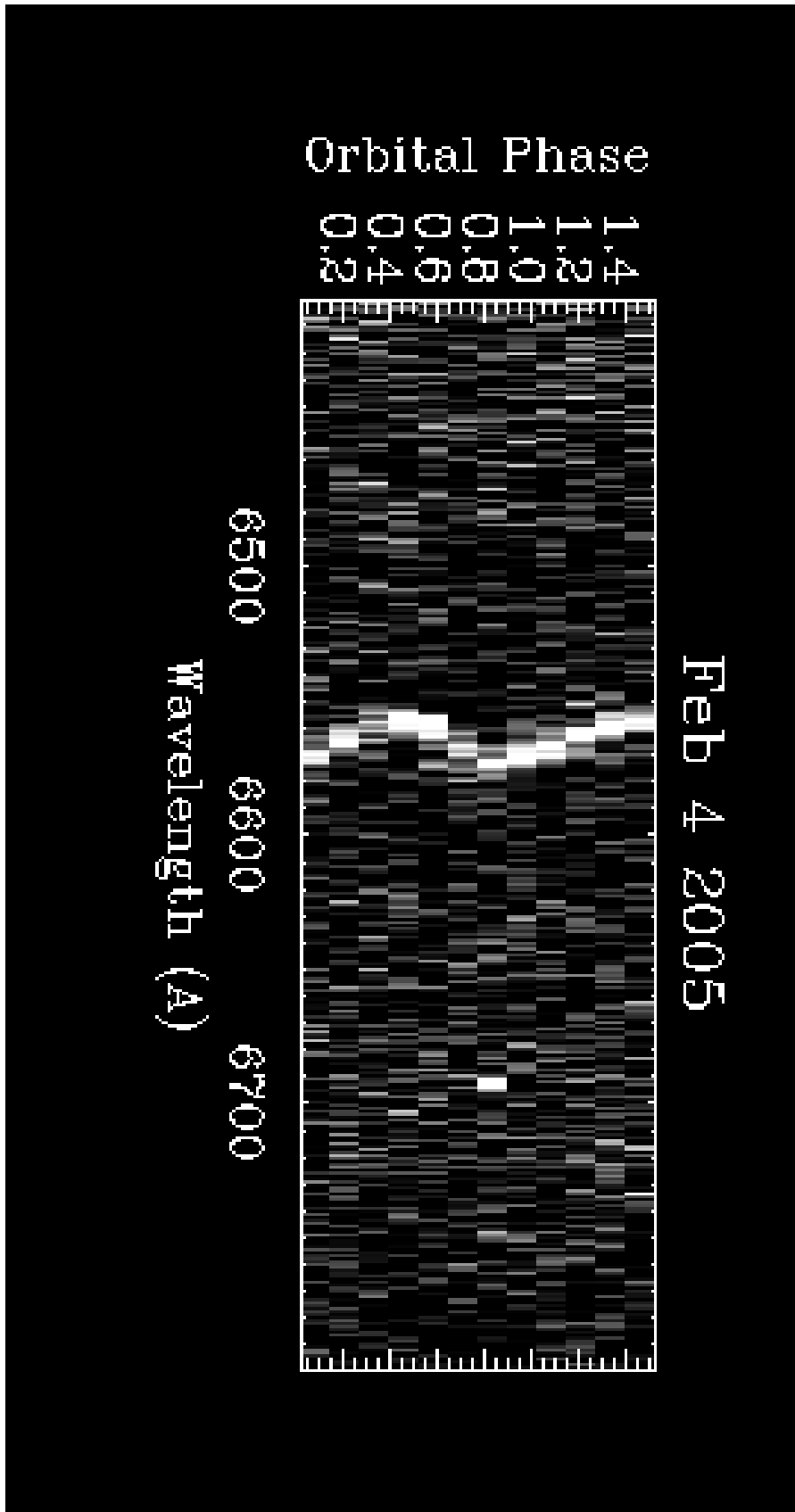


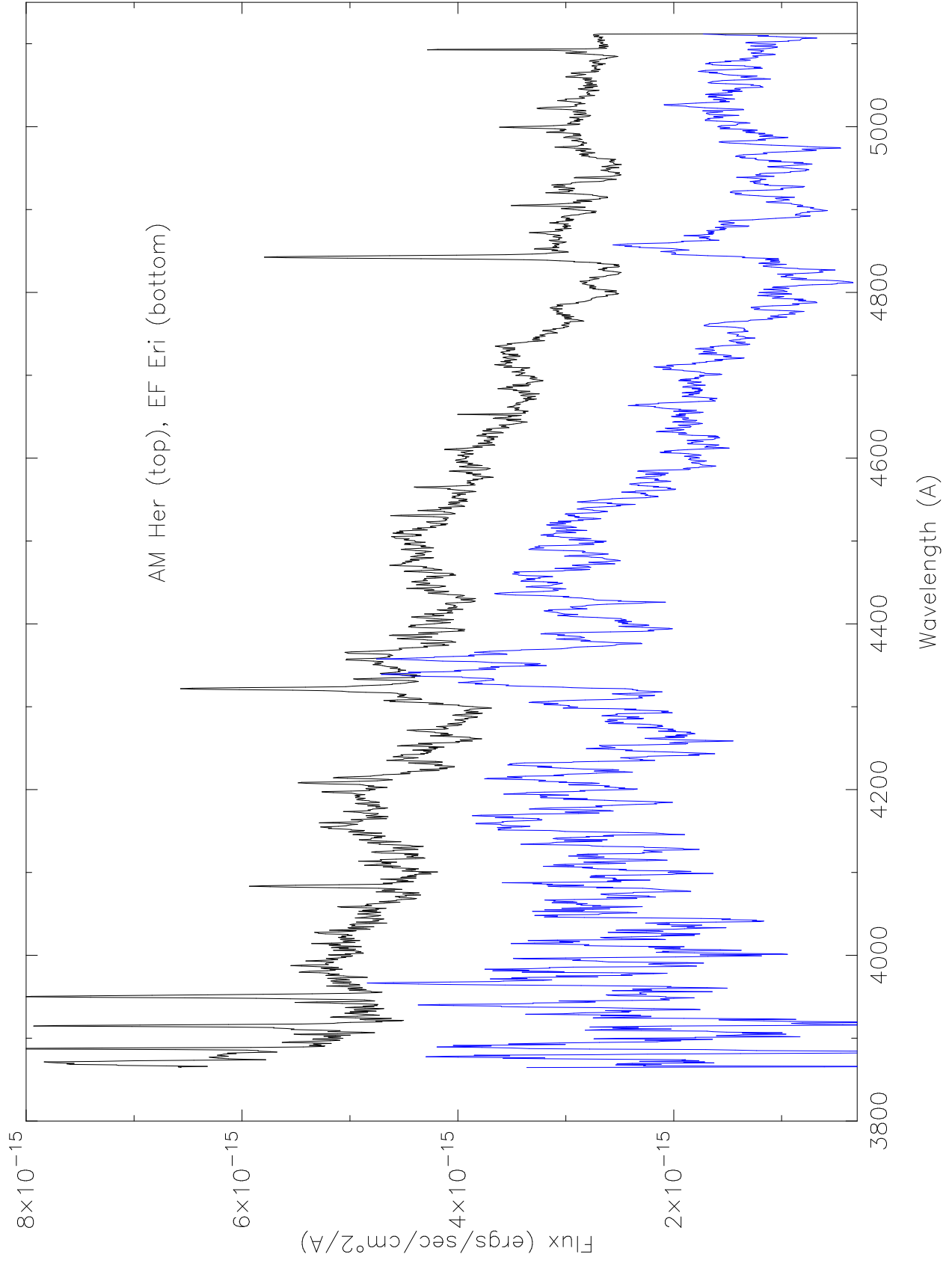


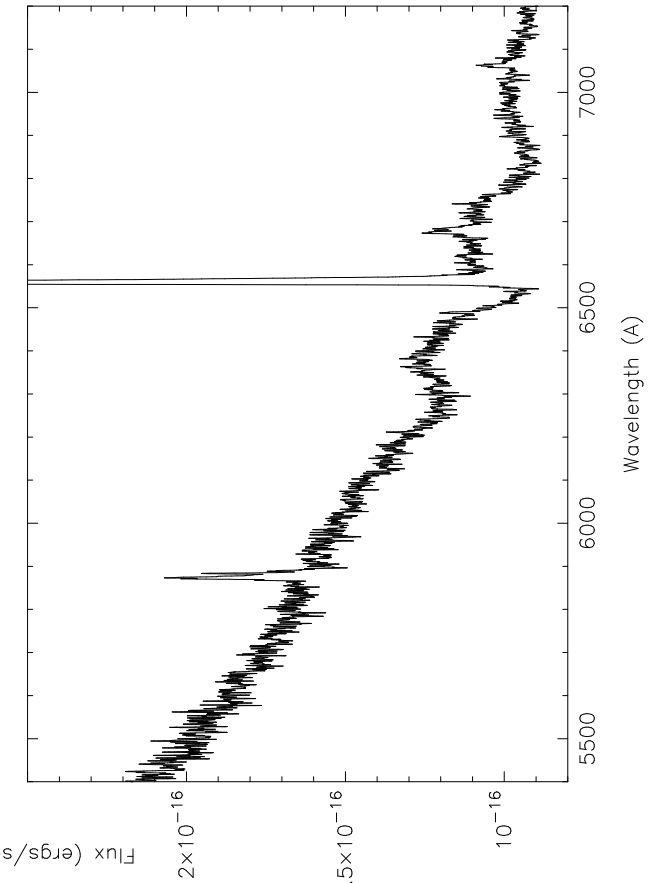
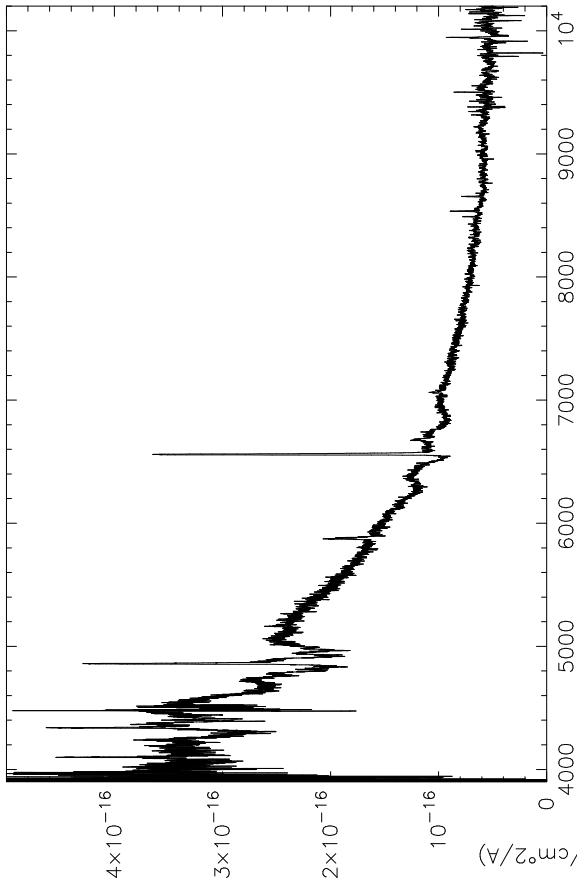
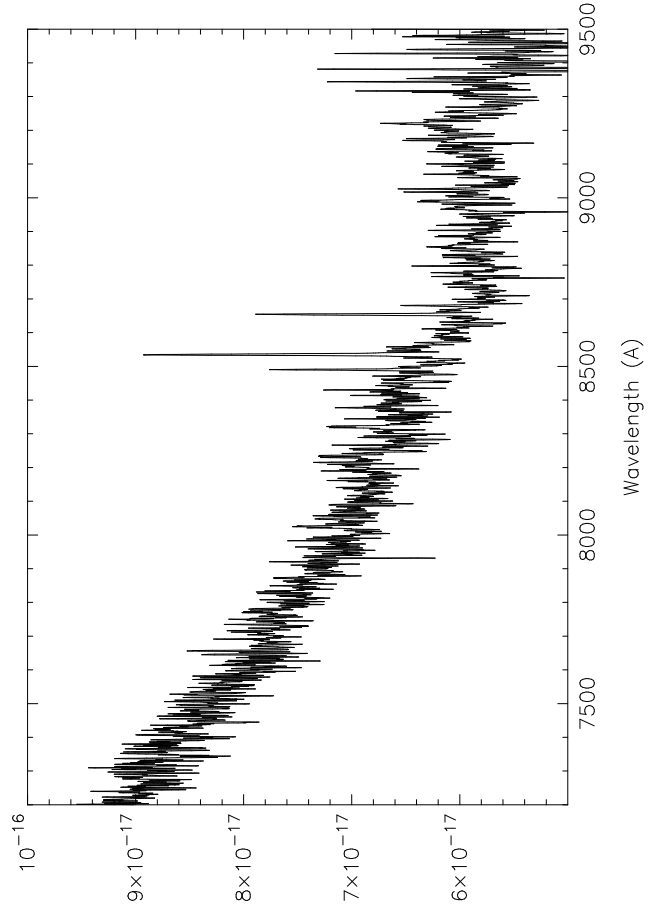
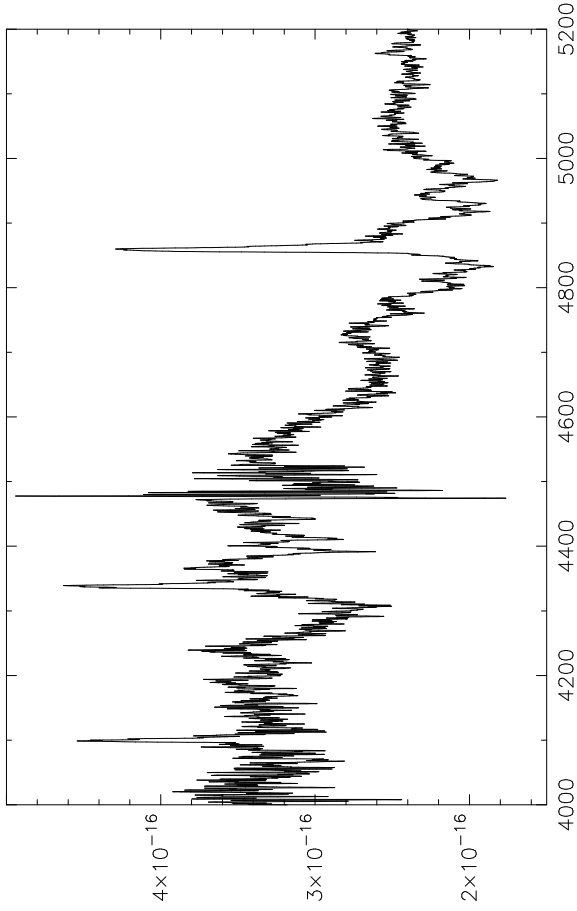


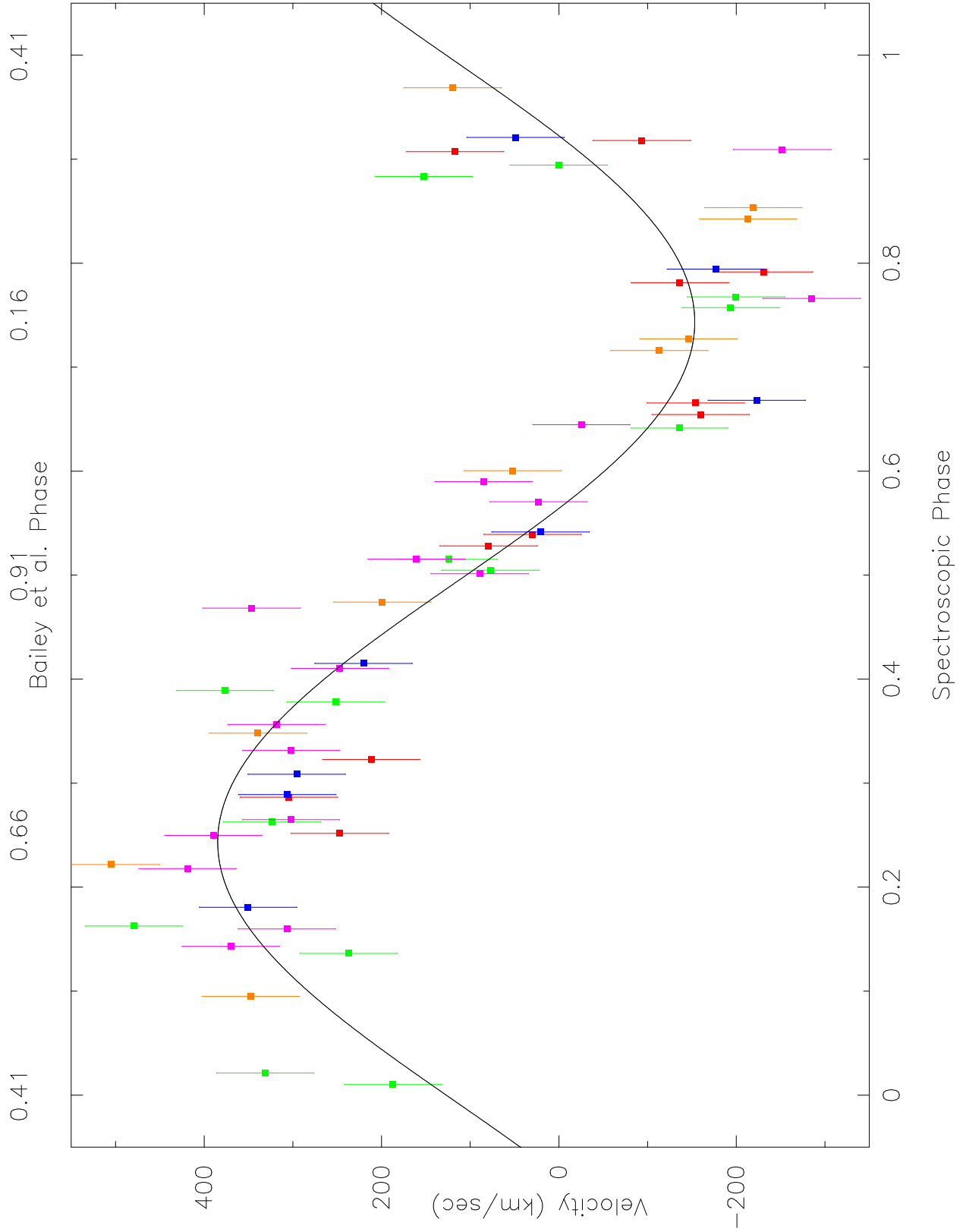


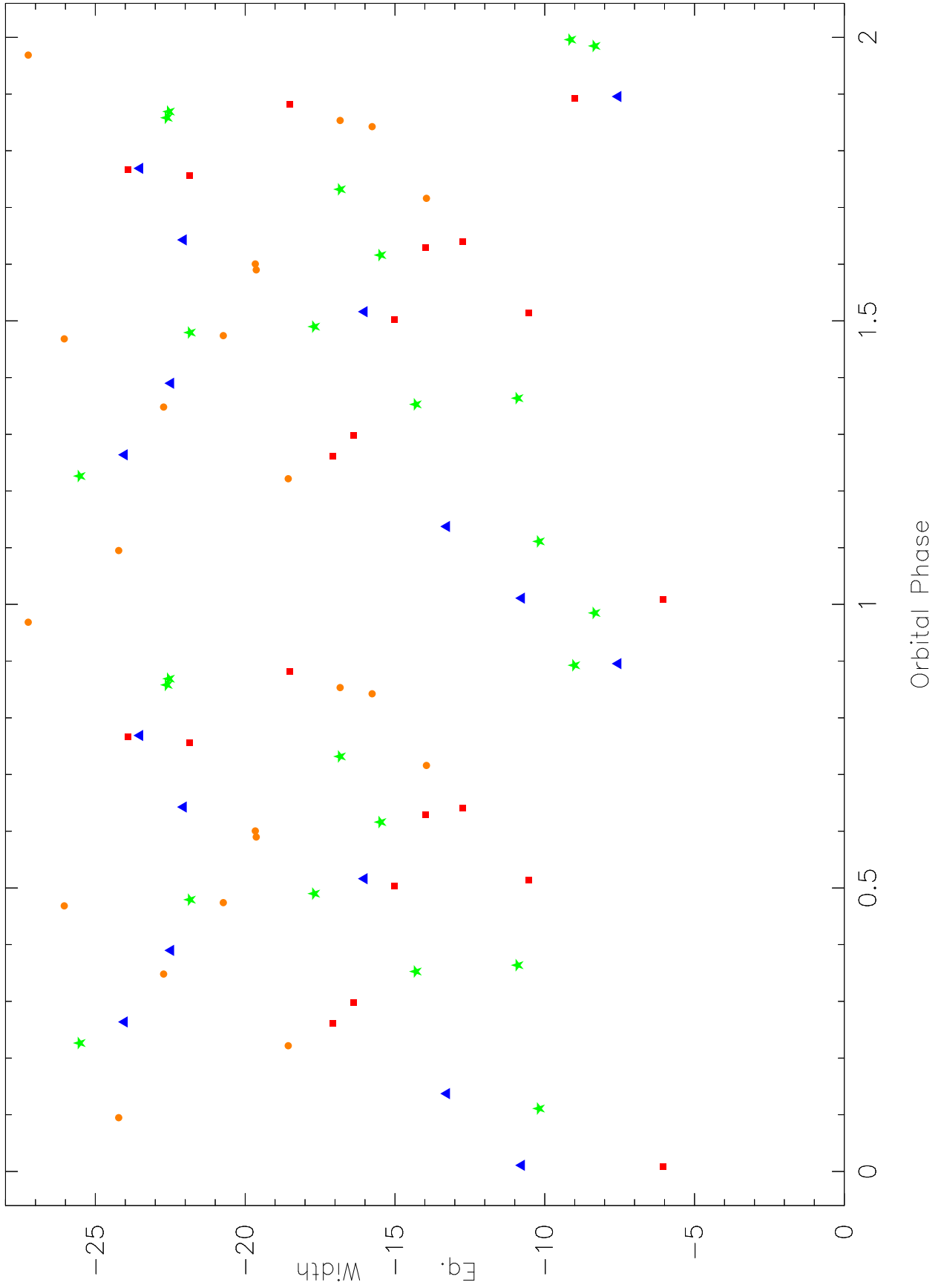


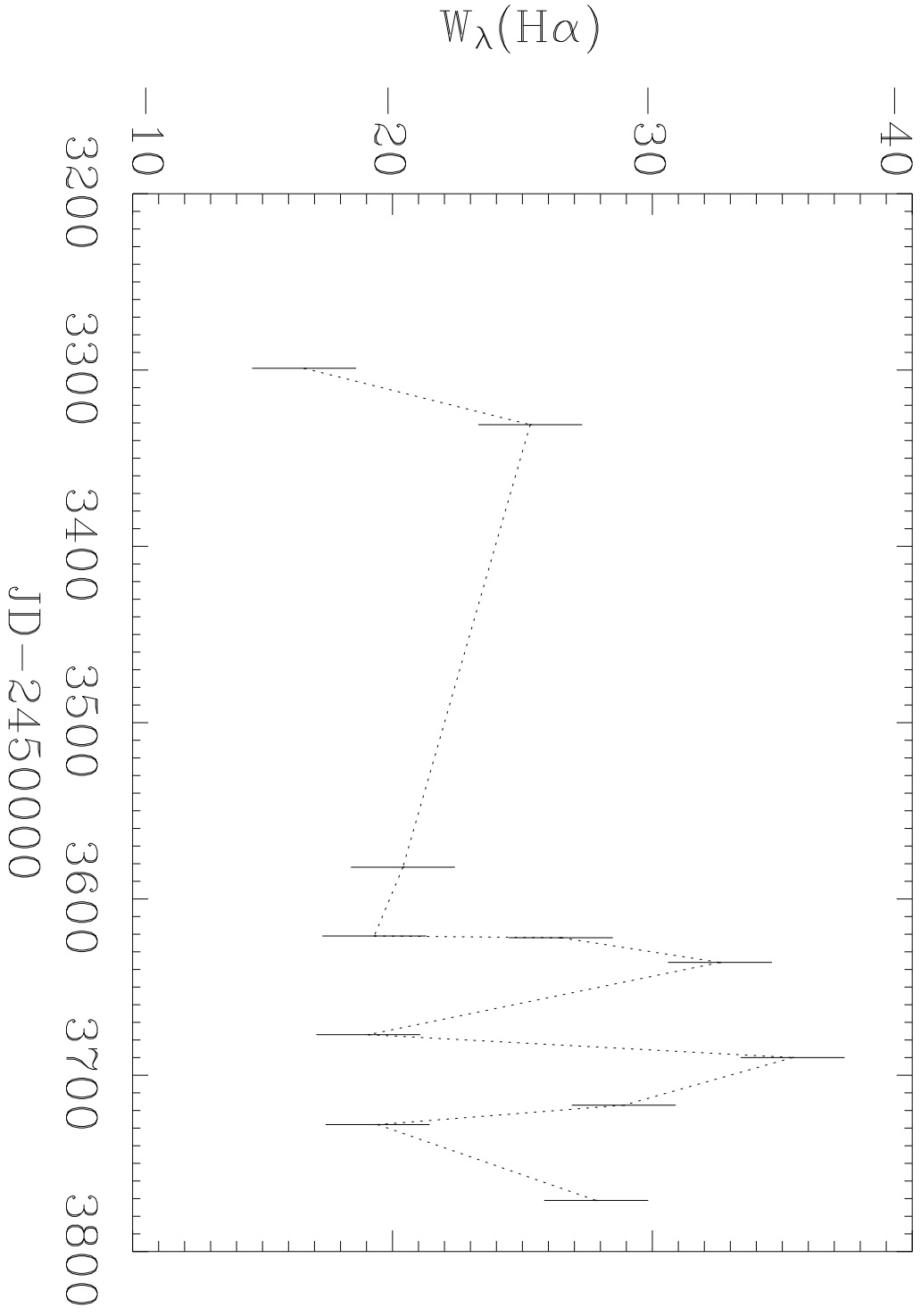


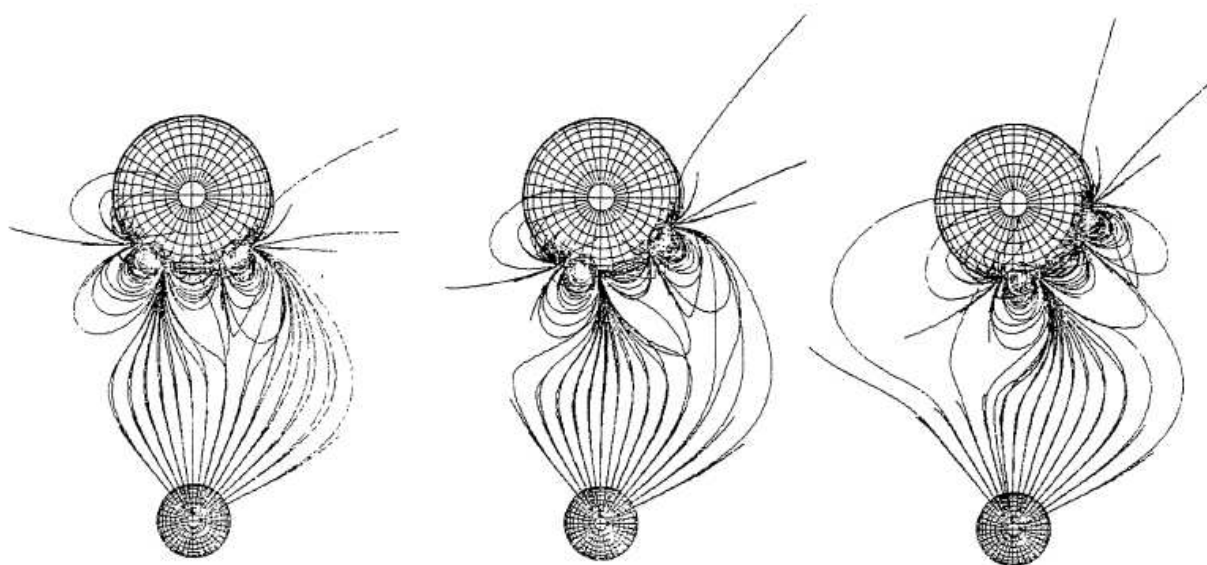


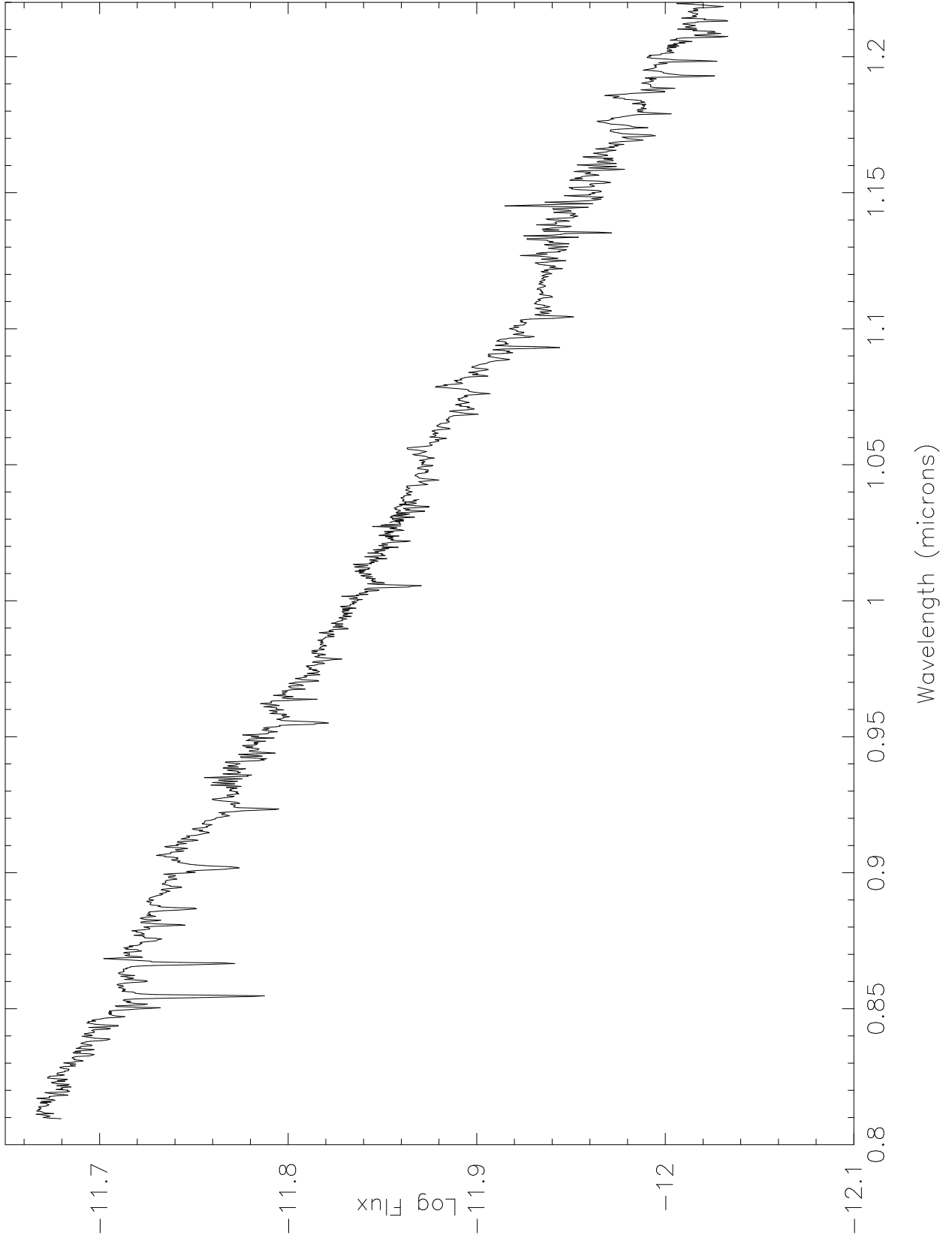


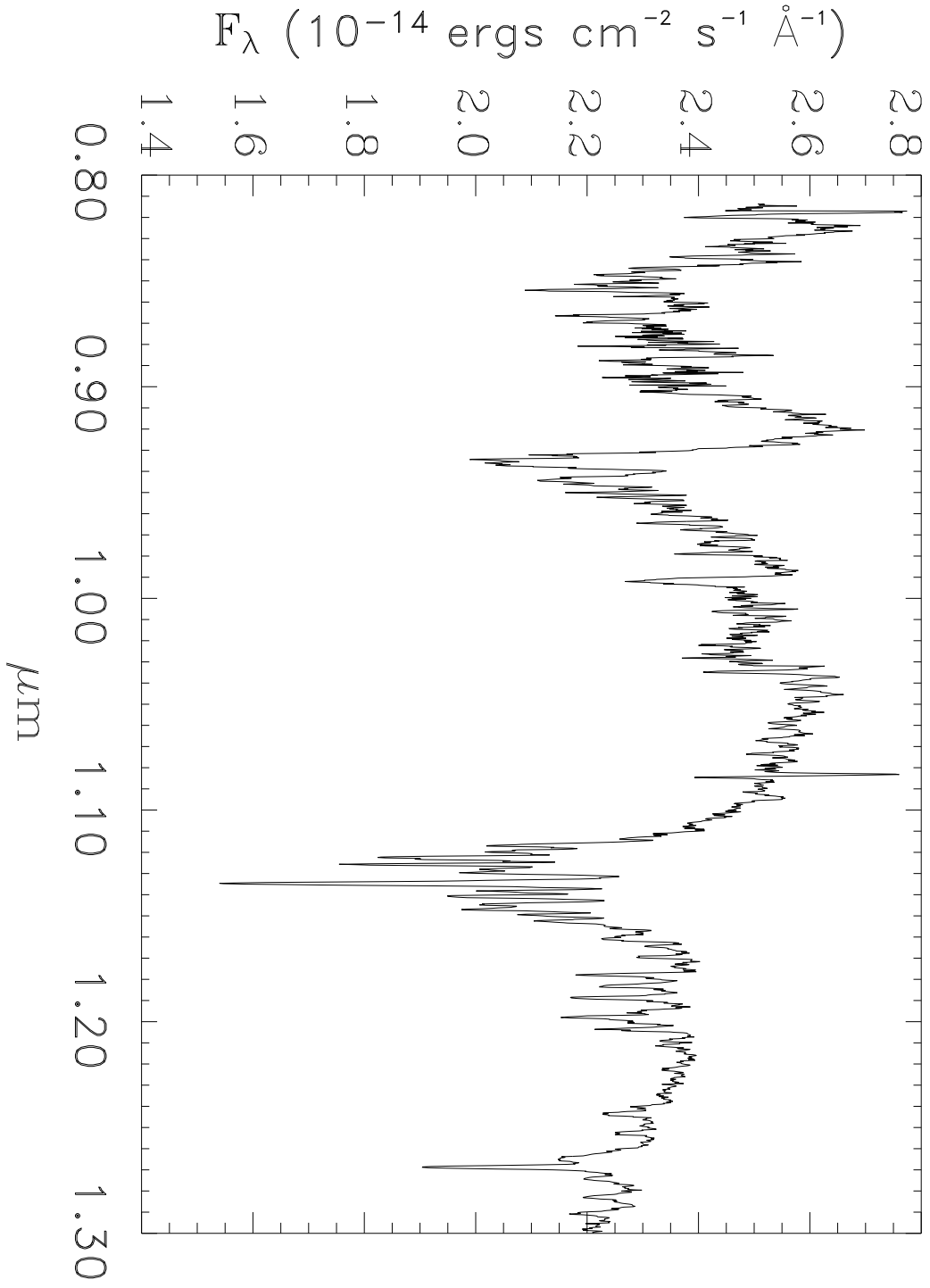












EF Eri

